

OFDMA-Based Channel-Width Adaptation in Wireless Mesh Networks

Xudong Wang, *Senior Member, IEEE*, Pengfei Huang, Jiang Xie, *Senior Member, IEEE*, and Mian Li

Abstract—Channel-width adaptation can optimize multiple performance metrics of a wireless communication link, including transmission rate, communication range, resilience to delay spread, and power consumption. Supporting variable channel width has been considered one of the most critical features of a communication radio. How to leverage a channel-width adaptive radio to improve throughput of a wireless network is a challenging problem in the medium access control (MAC) layer. So far, there exist research results on either theoretical analysis or protocol implementation for a point-to-multipoint (PMP) infrastructure network. However, the impact of channel width to a multihop wireless network has not been fully investigated yet. More specifically, how to exploit variable channel width to enhance throughput of a multihop wireless network remains an unresolved research issue. This paper addresses this issue in wireless mesh networks (WMNs) considering orthogonal frequency-division multiple-access (OFDMA)-based channel-width adaptation. Theoretical analysis is first carried out to identify appropriate algorithms for channel width adaptation. To this end, resource allocation with OFDMA-based channel-width adaptation is formulated as an optimization problem, which is proved to be NP-complete. To reduce the computational complexity, a greedy algorithm is derived to obtain a suboptimal solution. Based on such a greedy algorithm, a distributed MAC protocol is designed for channel-width adaptation for OFDMA-based WMNs. It takes advantage of variable channel width in different time slots to achieve highly efficient resource allocation. Simulation results illustrate that the distributed MAC protocol significantly outperforms MAC protocols based on traditional channel-width adaptation.

Index Terms—Channel-width adaptation, distributed medium access control (MAC) protocol, wireless mesh networks (WMNs).

I. INTRODUCTION

ADJUSTING channel width can optimize a few performance metrics of a wireless communication link. For example, given a certain level of transmission power, reducing the channel width of a wireless link can reliably increase its communication range; if the channel width is further reduced,

then the power consumption can be also decreased without compromising the communication range. Thus, channel-width adaptation can optimize both communication range and power consumption that are usually in conflict with each other in a wireless link with fixed channel width [1]. Considering another scenario where a vehicular network is built based on orthogonal frequency-division multiplexing (OFDM), when a vehicle moves from a rural area to a suburb area, the delay spread of its communication link may increase to a level larger than the guard interval of OFDM symbols; however, reducing channel width is effective to fix this problem [2].

Because of the benefits of channel-width adaptation, supporting multiple options of channel width in a communication radio has become a common practice. For example, many IEEE 802.11 chipsets made by Atheros (now part of Qualcomm) support channel widths of 5, 10, 20, and 40 MHz. Similarly, WiMAX and long-term evolution chipsets also support a set of different channel widths. However, how to utilize such communication radios to improve network performance is a nontrivial task because a wireless network usually involves many communication links that all demand channel-width adaptation. In a point-to-multipoint (PMP) wireless network such as the IEEE 802.11 basic service set in infrastructure mode or an extended PMP network such as the IEEE 802.11 extended service set, research work has been conducted to utilize channel-width adaptation. In [1], the advantages of channel-width adaptation are analyzed using commodity IEEE 802.11 radios. A simple channel-width adaptation algorithm is derived for the basic scenario of a single link with two communication nodes. In [3] and [4], the channel widths of all access points in the distribution system of an IEEE 802.11 network are optimized according to different traffic load distributions in each basic service set. As a result, the throughput and the fairness of bandwidth distribution of the entire IEEE 802.11 network are greatly enhanced [3], [4]. A general case of adaptive channel-width allocation in base stations considering the demands of clients is analyzed in [5], where throughput maximization is formulated as a maximum bipartite flow problem.

The channel-adaptation algorithms in [1] and [3]–[5] are not applicable to a multihop wireless network because they all assume that the network works in a single-hop infrastructure mode. For multihop wireless networks, there still lack channel-width adaptation algorithms. Different types of multihop wireless networks are characterized by different features, which leads to different requirements and challenges in channel-width adaptation. For example, in a mobile ad hoc network, channel-width adaptation can be utilized to compensate delay spread and increase link stability. However, since the network

Manuscript received August 3, 2013; revised November 23, 2013; accepted February 1, 2014. This work was supported in part by the National Natural Science Foundation of China under Grant 61172066, by the Oriental Scholar Program of Shanghai Municipal Education Commission, and by Shanghai Pujiang Scholar Program 10PJ1406100. The review of this paper was coordinated by Prof. Y. Qian.

X. Wang and M. Li are with the University of Michigan-Shanghai Jiao Tong University (UM-SJTU) Joint Institute, Shanghai Jiao Tong University, Shanghai 200240, China (e-mail: wxudong@ieee.org).

P. Huang is with the Department of Electrical and Computer Engineering, University of California at San Diego, La Jolla, CA 92093, USA.

J. Xie is with the University of North Carolina, Charlotte, NC 28223 USA.

Color versions of one or more of the figures in this paper are available online at <http://ieeexplore.ieee.org>.

Digital Object Identifier 10.1109/TVT.2014.2308316

89 topology is highly variable due to mobility, allocating different
 90 channel widths to different links is an extremely challenging
 91 task. In a wireless mesh network (WMN) [6], mobility is
 92 minimal. In particular, in the infrastructure of a WMN, all
 93 communication links remain stationary [6]. As a result, issues
 94 such as communication range, delay spread, and link stability
 95 can be considered during the network design and deployment
 96 phase. However, there exists one highly variable parameter
 97 that impacts the performance of WMNs, which is traffic load
 98 distribution on each link. It is rather common in WMNs that
 99 some links experience heavy traffic, whereas other links support
 100 only light traffic. To conduct efficient resource allocation for
 101 these links, a link with light traffic must be assigned with a very
 102 small resource unit, whereas a link with heavy traffic needs a
 103 large number of such resource units. If a time slot with fixed
 104 channel width is considered as a resource unit, then it is difficult
 105 to achieve the fine granularity of a small resource unit. For
 106 example, in many wireless networks, a link with fixed channel
 107 width can deliver a rate of 50 Mb/s or more; to achieve a
 108 resource unit of 100 Kb/s, the time slot length is 240 μ s when
 109 the frame size is 1500 bytes and can be as small as 24 μ s when
 110 the frame size is 150 bytes. Implementing such a small time slot
 111 is extremely challenging and can also result in large overhead
 112 due to the need of guard time. This problem can be properly
 113 solved by leveraging channel-width adaptation. More specifi-
 114 cally, a fine-grained resource unit can be achieved by reducing
 115 channel width in a time slot. Thus, in this paper, channel-width
 116 adaptation algorithms and protocols are developed to satisfy
 117 heterogeneous traffic demands on various links in WMNs.

118 Traditionally, channel width of a link can be adjusted by se-
 119 lecting different options (e.g., 5, 10, 20, and 40 MHz) available
 120 in a radio. To consider finer channel-width adaptation, orthogo-
 121 nal frequency-division multiple-access (OFDMA) is adopted.
 122 We consider a single-radio WMN, where each radio adopts
 123 OFDMA. The channel width in a time slot of each radio is ad-
 124 justed by selecting a different number of subchannels. Thus, the
 125 problem of channel-width adaptation to heterogeneous traffic
 126 demands in various links is converted to another problem, i.e.,
 127 how to allocate subchannels and time slots to different links of
 128 a WMN such that the throughput of the entire network is maxi-
 129 mized. We have made the following contributions in this paper.

- 130 1) Channel-width adaptation is proposed to resolve the issue
 131 of mismatch between link capacity and traffic demands.
 132 Instead of a traditional adaptation mechanism by choos-
 133 ing different available spectrum (i.e., frequency center
 134 and frequency bandwidth), OFDMA-based channel-
 135 width adaptation is proposed as a new mechanism. Based
 136 on this new mechanism, the channel-width adaptation
 137 problem in WMNs is converted into a time slot and
 138 subchannel allocation problem.
- 139 2) An optimization problem is formulated to investigate the
 140 channel-width adaptation problem in WMNs. The corre-
 141 sponding decision problem of this optimization problem
 142 is proved to be NP-complete, which reveals the complex-
 143 ity of channel-width adaptation in WMNs. To reduce the
 144 complexity, a greedy algorithm is proposed to obtain a
 145 suboptimal solution. With the feasible solution from the

greedy algorithm as the initial population, a genetic algo- 146
 rithm (GA) is derived to obtain a near-optimal solution. 147
 Taking the GA as a reference, the greedy algorithm is 148
 shown to achieve comparable performance as that of a 149
 near-optimal solution. 150

- 3) It is shown that the greedy algorithm can be executed 151
 in a distributed way. Thus, this algorithm is incorporated 152
 into a distributed medium access control (MAC) protocol 153
 for channel-width adaptation in OFDMA WMNs. The 154
 MAC protocol is highly adaptive to dynamic network 155
 conditions such as variable traffic demands of wireless 156
 links. Thus, the throughput of the entire network is greatly 157
 improved. 158

The remainder of this paper is organized as follows. The 159
 basic mechanisms and benefits of channel-width adaptation 160
 based on OFDMA are explained in Section II, where related 161
 work is also presented. The time slot and subchannel allo- 162
 cation problem for channel-width adaptation is formulated in 163
 Section III, where a greedy algorithm and a GA are devel- 164
 oped to obtain a near-optimal solution to resource allocation. 165
 Based on the greedy algorithm, a distributed MAC protocol is 166
 designed in Section IV. Performance results are presented in 167
 Section V, and the paper is concluded in Section VI. 168

169 II. CHANNEL-WIDTH ADAPTATION BASED ON 169 170 ORTHOGONAL FREQUENCY-DIVISION MULTIPLE-ACCESS: 170 171 MECHANISMS, BENEFITS, AND RELATED WORK 171

172 A. OFDMA-Based Channel-Width Adaptation Mechanisms 172

We consider a single-radio WMN. Traditionally, the channel 173
 width of a link can be adjusted by selecting: 1) different options 174
 of channel width (e.g., 5, 10, 20, and 40 MHz) available in a ra- 175
 dio; and 2) the center frequency of the operation channel spec- 176
 trum. However, the performance of this approach is impacted 177
 by several drawbacks. First, the granularity of channel-width 178
 adjustment is constrained, and thus, the step size of channel- 179
 width adjustment is limited. For example, the minimum channel 180
 width in an IEEE 802.11 radio must be 5 MHz and the step 181
 size is 5, 10, or 20 MHz. Second, the operation spectrum of a 182
 channel on a radio must be consecutive. 183

In this paper, a different approach is proposed to adjust 184
 channel width. It is based on the capability of subchannels (i.e., 185
 a number of subcarriers) allocation of OFDMA. Compared with 186
 a radio with traditional channel-width adaptation, an OFDMA- 187
 based radio brings several advantages. 188

- 1) It is flexible to adjust channel width to support traffic 189
 demand by selecting a different number of subchannels. 190
- 2) It does not require the spectrum of the selected subchan- 191
 nels to be consecutive, and the step size of channel-width 192
 adaptation can be as fine as one subchannel. 193
- 3) A single OFDMA radio node can support multiple com- 194
 munication links at the same time. 195

196 B. Benefits of the OFDMA-Based Channel-Width Adaptation 196

The benefits of the OFDMA-based channel-width adaptation 197
 are demonstrated in the following example. 198

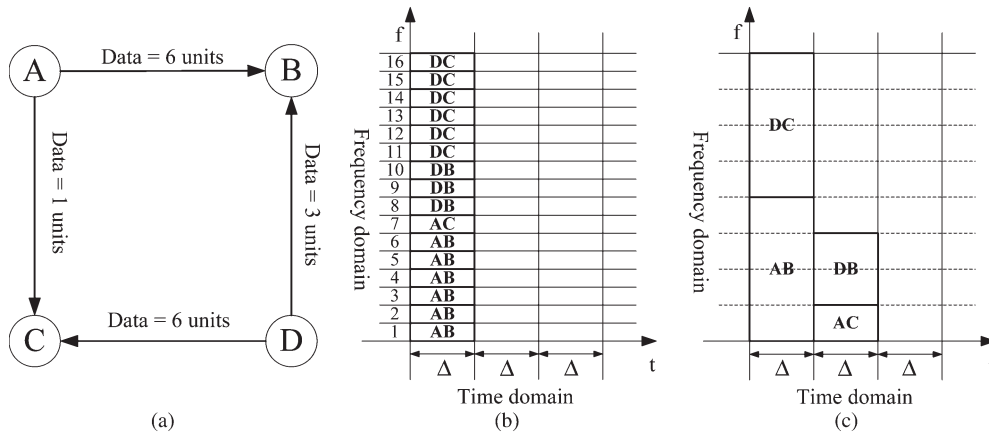


Fig. 1. Benefits of the OFDMA-based channel-width adaptation scheme. (a) Communication topology. (b) OFDMA-based scheme. (c) Traditional scheme.

199 A simple WMN with four nodes A , B , C , and D is consid-
 200 ered in Fig. 1(a), where each node is equipped with one radio.
 201 The links are directional, and the whole spectrum is assumed
 202 to be 40 MHz. In the case of the OFDMA-based channel-width
 203 adaptation mechanism, the whole spectrum is divided into
 204 16 subchannels. For the traditional channel-width adaptation
 205 scheme, channel width can only be selected from $\{5, 10, 20,$
 206 $40\}$ MHz, but the center frequency of a channel can be arbitrar-
 207 ily adjusted. We assume that subchannels are allocated to nodes
 208 slot by slot, and one subchannel per time slot Δ can convey
 209 1 unit traffic demand. In Fig. 1(a), the traffic demands in links
 210 AB , AC , DB , and DC are 6, 1, 3, and 6 units, respectively.

211 Considering the OFDMA-based channel-width adaptation
 212 scheme, the subchannel and time slot allocation is shown in
 213 Fig. 1(b). To support all traffic demands, the time-division
 214 multiple-access (TDMA) frame can be as short as Δ , and the
 215 throughput of the network is $(6 + 1 + 3 + 6)/1 = 16$ (units/ Δ).
 216 Considering the traditional channel-width adaptation scheme,
 217 the channel and time slot allocation is shown in Fig. 1(c). To
 218 support all traffic demands, the TDMA frame needs to be 2Δ .
 219 Thus, the throughput of the network is $(6 + 1 + 3 + 6)/2 =$
 220 8 (units/ Δ).

221 This simple example demonstrates that the network through-
 222 put can be greatly improved by the OFDMA-based channel-
 223 width adaptation scheme for the following reasons: 1) An
 224 OFDMA radio can support several communication links simul-
 225 taneously; and 2) the granularity of channel-width adjustment
 226 of an OFDMA radio can be as small as a subchannel.

227 However, two issues specific to OFDMA-based channel-
 228 width adaptation need to be considered: 1) channel-width
 229 adaptation in both frequency domain and time domain, i.e.,
 230 both time slot and subchannel allocation; and 2) *transmitting*
 231 and *receiving constraint*, i.e., in a time slot, the subchannels
 232 allocated to a radio can only be used for either transmitting or
 233 receiving packets because full duplex wireless communications
 234 [7] are not considered in the OFDMA radio.

235 C. Related Work

236 So far many research papers have addressed the channel
 237 allocation problem in WMNs. For papers on single-radio mul-
 238 tichannel operation [8]–[10], their results are not applicable

to the OFDMA-based channel-width adaptation because fixed
 239 channel width is assumed. For papers on multiradio multichan-
 240 nel operation [11], [12], their algorithms cannot be adopted
 241 either because in the OFDMA-based channel-width adaptation,
 242 there exists a constraint that each node can either transmit
 243 or receive packets on subchannels at one time slot, whereas
 244 this constraint is not considered in the multiradio multichannel
 245 scenarios. In [13], a different channel width is available through
 246 channel combining on a radio for the WMNs. However, the
 247 approach explained in [13] is different from our OFDMA-based
 248 scheme in a single-radio WMN in two aspects: 1) In [13], one
 249 node can only maintain one communication link. However, in
 250 our scheme, one node can simultaneously support several com-
 251 munication links with different nodes; and 2) in [13], a radio
 252 can only use continuous channels, but a radio in our scheme
 253 can transmit on any subchannels in the communication band.
 254 To date, there also exist research results on subcarrier allocation
 255 for OFDMA WMNs. In [14], fair allocation of subcarrier and
 256 power is studied for a specific WMN with one mesh router and
 257 multiple mesh clients. Thus, their point-to-many-points (PMP)
 258 structure is different from our ad hoc network model. In [15],
 259 a joint power-subcarrier-time allocation algorithm is derived
 260 for one cluster of a WMN. In each cluster, the mesh router
 261 is responsible for resource assignment for its mesh clients.
 262 Thus, their network structure is also PMP. More recently, the
 263 resource-allocation problem of multihop OFDMA WMNs has
 264 been conducted in [16]–[19]. However, these papers focus on a
 265 relay-based two-hop network model. Thus, their algorithms are
 266 not applicable to a generic WMN. Consequently, to solve the
 267 subchannel allocation problem for channel-width adaptation in
 268 generic WMNs, new resource-allocation algorithms need to be
 269 derived and an appropriate one must be identified to conduct
 270 channel-width adaptation in a distributed MAC protocol, which
 271 is the focus of this paper. 272

273 III. CHANNEL-WIDTH ADAPTATION ALGORITHMS BASED 274 ON ORTHOGONAL FREQUENCY-DIVISION 275 MULTIPLE-ACCESS 275

Here, the resource-allocation problem considering channel-
 276 width adaptation is formulated first, and then the corresponding
 277 greedy and GAs are derived. 278

279 A. Problem Formulation

280 We consider a WMN consisting of N nodes and L directional
281 links. Each node is equipped with an OFDMA radio. The
282 transmission range of each node is R , and the interference range
283 is R' . The network is modeled as a directional communication
284 graph $G(V, A)$, where V is a set of nodes and A is a set of
285 directed edges. Moreover, $|V| = N$ and $|A| = L$. Thus, for link
286 $l(i, j) \in A$, node $i \in V$ is specified as the sending node and
287 node $j \in V$ is the receiving node.

288 OFDMA is considered in the WMN; hence, a resource unit
289 is a subchannel in a certain time slot. The length of a time slot
290 is fixed, but the TDMA frame length is variable according to
291 the fluctuating traffic demands of all links in the WMN. More
292 specifically, when resource allocation is performed, the total
293 number of time slots is determined such that traffic demands
294 of all links are satisfied within a TDMA frame. This design
295 eliminates the need of admission control, which is a preferred
296 feature of data networks. To be consistent with this design, the
297 traffic demand of a link is not specified as the actual traffic
298 load. Instead, it is specified as the number of resource units per
299 TDMA frame, and each unit represents the data transmitted in
300 one subchannel per time slot, which is the same as the definition
301 in Section II-A. For easy specification of traffic demands, when
302 a node needs to specify the traffic demand of a link, it selects
303 a traffic demand level from the set of $\{1, 2, \dots, M\}$ (units),
304 and the selected level is proportional to its expected actual
305 traffic load. This design of the TDMA frame structure and the
306 resource-allocation mechanism achieves time slotted resource
307 sharing among links of all nodes, which is well suited for data
308 networks.

309 In our OFDMA-based channel-width adaptation mechanism,
310 it is assumed that the whole spectrum is divided into W
311 subchannels and one subchannel supports one unit of traffic
312 demand per time slot. The OFDMA-based radio can transmit
313 data on any combination of these subchannels.

314 We use the protocol model [20] as the interference model.
315 Under this model, a transmission from node i to node j in a time
316 slot is successful if two conditions are satisfied: 1) $d_{ij} \leq R$,
317 where d_{ij} is the distance between node i and node j ; 2) any
318 node k that occupies at least one overlapping subchannel with
319 link $l(i, j)$ and $d_{kj} \leq R'$ is not transmitting. Moreover, a unit
320 of traffic demand means the equivalent data rate that can be
321 supported by a subchannel per time slot. Although the physical
322 layer parameters (such as channel gain and rate adaptation) can
323 impact the data rate of a subchannel per time slot, such impact
324 can be captured by different units of traffic demand. In other
325 words, given the same traffic load, the equivalent units of traffic
326 demand are higher for a lower rate subchannel. Thus, physical
327 layer parameters are not explicitly considered in the protocol
328 model. Due to the OFDMA technique, the problem of channel-
329 width adaptation can be converted into a resource-allocation
330 problem: given traffic demands on different links, how time
331 slots and subchannels are assigned under some constraints such
332 that the total traffic demands are satisfied with the least number
333 of time slots, i.e., the network throughput is maximized. This
334 resource-allocation problem is formulated as follows. First, our
335 objective is to minimize the number of time slots (i.e., the

length of one TDMA frame) that can support the given traffic 336
demands. Suppose that the total number of time slots consumed 337
by the WMN is denoted as T , then the objective function 338
becomes 339

$$\text{Minimize } T. \quad (1)$$

Obviously, T lies in the positive integer set, i.e., 340

$$T \in \{1, 2, \dots\}. \quad (2)$$

To help determine time slot and subchannel allocation for 341
each directional link, $X(i, j, t, s)$ is used to denote the alloca- 342
tion status of link $l(i, j)$ in time slot t and subchannel s . Since 343
 $X(i, j, t, s) \in \{0, 1\}$, we have the following constraint: 344

$$\begin{aligned} X(i, j, t, s) &\in \{0, 1\} \\ \forall l(i, j) \in A \quad \forall t = 1, 2, \dots, T \quad \forall s = 1, 2, \dots, W. \end{aligned} \quad (3)$$

To capture potential interference between links, we need a 345
link interference constraint described as follows: 346

$$\begin{aligned} X(i, j, t, s) + X(p, q, t, s) &\leq 1 \\ \forall l(i, j) \in A \quad \forall t = 1, 2, \dots, T \quad \forall s = 1, 2, \dots, W \\ \forall l(p, q) \in I_{l(i, j)} \end{aligned} \quad (4)$$

where $I_{l(i, j)}$ is the interference set of link $l(i, j)$. 347

Since each mesh node has a single radio, it either transmits 348
or receives on all the occupied subchannels in the same time 349
slot. Thus, for a certain link $l(i, j)$, we have the following 350
transmitting and receiving constraint (i.e., *Tx/Rx constraint*): 351

$$\begin{aligned} X(i, j, t, s) \times \left[X(i, j, t, s) + \sum_{f=1}^W \sum_{p \in \text{in}(i)} X(p, i, t, f) \right. \\ \left. + \sum_{g=1}^W \sum_{q \in \text{out}(j)} X(j, q, t, g) \right] &\leq 1 \\ \forall l(i, j) \in A \quad \forall t = 1, 2, \dots, T \quad \forall s = 1, 2, \dots, W \end{aligned} \quad (5)$$

where $\text{in}(i)$ is a set of nodes that send data to node i . Similarly, 352
 $\text{out}(j)$ is the set of nodes that receive data from node j . 353

Finally, to satisfy the traffic demand of each link $l(i, j) \in A$, 354
we need to consider the *traffic demand constraint* 355

$$\begin{aligned} \sum_{t=1}^T \sum_{s=1}^W X(i, j, t, s) &\geq D(i, j) \\ D(i, j) &\in \{1, 2, \dots, M\} \end{aligned} \quad (6)$$

where $D(i, j)$ represents the units of traffic demand on link 356
 $l(i, j)$. This constraint means that each link must be assigned 357
with enough time slots and subchannels to support its traffic 358
demand. 359

Consequently, we have formulated the optimization problem 360
of time slot and subchannel allocation for OFDMA-based 361
channel-width adaptation. We call this problem the single- 362
radio OFDMA-based resource-allocation (SRORA) problem. 363
In summary, SRORA needs to optimize the objective in (1), 364
subject to constraints in (2)–(6). In the following theorem, we 365
prove that SRORA is NP-complete. 366

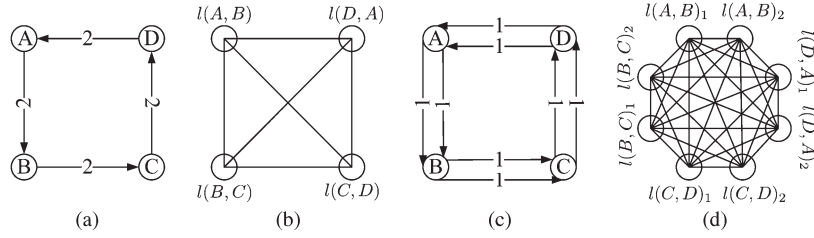


Fig. 2. (a) Communication graph $G(V, A)$, which consists of four directional communication links. Each link has 2 units of traffic demands. Based on the protocol interference model, $G(V, A)$ is converted into the interference graph G' in (b), where each vertex represents a directional communication link in $G(V, A)$. (c) Split communication graph of $G(V, A)$. It is constructed by splitting a communication link in $G(V, A)$ into several links, each with one unit of traffic demand, e.g., $l(A, B)$ in $G(V, A)$ has two units of traffic demands; hence, it is split into $l(A, B)_1$ and $l(A, B)_2$ in G_{split} , each with one unit of traffic demand. (d) Interference graph of the split communication graph G_{split} . (a) $G(V, A)$. (b) G' . (c) G_{split} . (d) G'_{split} .

367 *Theorem 1:* In SRORA, the decision problem of verifying
368 whether K time slots are enough to satisfy the total traffic
369 demands is NP-complete.

370 *Proof:* First, for any candidate solution of time slot and
371 subchannel allocation, whether all the constraints are satisfied
372 can be verified in polynomial time. Thus, the decision problem
373 in SRORA is NP. Second, we consider the special case of
374 SRORA by setting $W = 1$ and $D(i, j) = 1$ for all links. Using
375 the protocol interference model, we convert the directional link
376 $l(i, j) \in A$ in the communication graph $G(V, A)$ into the vertex
377 in the corresponding interference graph G' , as shown in Fig. 2.
378 Based on the interference graph G' , each link $l(i, j)$ in the
379 communication graph $G(V, A)$ can construct an interference set
380 $I_{l(i, j)}$. Since in this special case only one subchannel and one
381 unit of traffic demand are considered for each link, only one
382 time slot is needed in a frame to satisfy *traffic demand con-*
383 *straint* (6). To satisfy *link interference constraint* (4), any link
384 in $I_{l(i, j)}$ must be assigned a different time slot from that of link
385 $l(i, j)$. In this special case, when *link interference constraint* (4)
386 is satisfied, *Tx/Rx constraint* (5) is also automatically satisfied
387 due to the two facts: 1) The links $l(p, i)$ where $p \in \text{in}(i)$ and
388 links $l(j, q)$ where $q \in \text{out}(j)$ are in set $I_{l(i, j)}$; and 2) the
389 link in $I_{l(i, j)}$ is assigned with a different time slot from the
390 link $l(i, j)$. Therefore, the problem of determining whether K
391 time slots are enough to support the traffic demands of all
392 links in the communication graph $G(V, A)$ is equivalent to the
393 problem of checking whether K colors are sufficient to color
394 the vertices in the corresponding interference graph G' . We
395 know that the latter problem is NP-complete [21], which means
396 that every problem in NP is reducible to the decision problem of
397 SRORA in polynomial time. As a result, the decision problem
398 of SRORA (in the special case) is NP-complete. In the general
399 case (with W subchannels and $D(i, j)$ traffic demand), the
400 decision problem is also NP-complete. \square

401 B. Greedy Algorithm

402 Since the problem SRORA is NP-complete, a low-
403 complexity greedy algorithm is proposed for the SRORA prob-
404 lem, and we call it GR-SRORA. In our greedy algorithm, links
405 are assigned with time slot and subchannel in a certain sequen-
406 tial order just like coloring the vertices in the corresponding
407 interference graph. However, here we also need to consider
408 *Tx/Rx constraint*.

GR-SRORA is described in Algorithm 1. It works as 409
follows. 410

- 411 1) Lines 2–15 specify the procedures of assigning the 411
time slot and subchannel to link $l(i, j)$ considering both 412
link interference constraint and *Tx/Rx constraint*. The 413
resource-allocation status table of link $l(i, j)$, denoted by 414
 $\Phi(i, j, t, s)$, captures *link interference constraint*. More 415
specifically, for any t and s , if $\Phi(i, j, t, s) = 1$, it means 416
that subchannel s in time slot t is occupied by a link in 417
the interference set of link $l(i, j)$ (i.e., $I_{l(i, j)}$). The single- 418
radio OFDMA constraint table of link $l(i, j)$, denoted by 419
 $\Psi(i, j, t)$, captures *Tx/Rx constraint*. More specifically, 420
for any t , if $\Psi(i, j, t) = 1$, it means that link $l(i, j)$ cannot 421
transmit on any subchannel in time slot t . 422
- 423 2) Lines 16–19 are executed after a link assignment. Two ta- 423
bles ($\Phi(p, q, t, s)$ and $\Psi(p, q, t)$) of each link are updated 424
and will be used in the next link assignment. 425
- 426 3) Line 21 is used to determine T_{greedy} , which is the total 426
number of time slots consumed by the network following 427
the greedy algorithm. 428

The performance of the greedy algorithm GR-SRORA is 429
analyzed as follows. We denote the minimum number of time 430
slots consumed in SRORA and the greedy algorithm GR- 431
SRORA as T_{optimal} and T_{greedy} , respectively. Based on the 432
split graph G_{split} of the original communication graph $G(V, A)$ 433
and the split interference graph G'_{split} in Fig. 2, the relationship 434
between T_{optimal} and T_{greedy} is shown in Theorem 2. 435

Algorithm 1 GR-SRORA

Input:

- Communication graph $G(V, A)$ 438
- Resource consumption status table of link $l(i, j)$: 439
 $\Phi(i, j, t, s)$ 440
- Single-radio OFDMA constraint table of link $l(i, j)$: 441
 $\Psi(i, j, t)$ 442
- Traffic demand on link $l(i, j)$: $D(i, j)$ 443
- Number of total subchannels: W 444

Output:

- Network time slot consumption: T_{greedy} 445
- The maximum time slot assigned to link $l(i, j)$: $T_{l(i, j)}$ 447
- Time slot and subchannel allocation result for link $l(i, j)$: 448
 $X(i, j, t, s)$ 449

450 **Initialization:**
451 • $\Phi(i, j, t, s) = 0$
452 • $\Psi(i, j, t) = 0$
453 • $T_{\text{greedy}} = 0$
454 • $T_{l(i,j)} = 0$

455 1: **for all** $l(i, j) \in A$ **do**
456 2: **for** $t = 1$ to $+\infty$ **do**
457 3: **if** $D(i, j) == 0$ **then**
458 4: **Break;**
459 5: **end if**
460 6: **if** $\Psi(i, j, t) \neq 1$ **then**
461 7: **for** $s = 1$ to W **do**
462 8: **if** $D(i, j) > 0$ && $\Phi(i, j, t, s) == 0$ **then**
463 9: $X(i, j, t, s) = 1$
464 10: $D(i, j) = D(i, j) - 1$
465 11: $T_{l(i,j)} = t$
466 12: **end if**
467 13: **end for**
468 14: **end if**
469 15: **end for**
470 16: **for all** $l(p, q) \in A$ **do**
471 17: Update $\Phi(p, q, t, s)$
472 18: Update $\Psi(p, q, t)$
473 19: **end for**
474 20: **end for**
475 21: $T_{\text{greedy}} = \max_{l(i,j) \in A} T_{l(i,j)}$
476 22: **Stop.**

477 *Theorem 2:* For the optimal solution of the problem SRORA
478 T_{optimal} and the greedy solution of GR-SRORA T_{greedy} ,
479 $\lceil (\chi(G'_{\text{split}})/W) \rceil \leq T_{\text{optimal}} \leq T_{\text{greedy}} \leq T_{\text{max}} = \delta(G'_{\text{split}}) + 1$,
480 where $\lceil \cdot \rceil$ is the ceiling function, $\delta(\cdot)$ is the maximum degree
481 of a graph, and $\chi(\cdot)$ is the chromatic number of a graph. More-
482 over, G'_{split} is the interference graph constructed by splitting a
483 communication link in $G(V, A)$ into separate links, each with
484 one unit traffic demand.

485 *Proof:* The proof consists of two parts. First, we derive
486 the lower bound of T_{optimal} by looking into the property of
487 T_{optimal} . In the communication graph $G(V, A)$, each directional
488 link $l(i, j)$ (with traffic demand $D(i, j)$) is split into $D(i, j)$ vir-
489 tual directional links between node i and node j to construct the
490 split communication graph G_{split} , as shown in Fig. 2(c). Based
491 on the protocol interference model, the split communication
492 graph G_{split} is converted into its corresponding interference
493 graph G'_{split} , as shown in Fig. 2(d). If each vertex of G'_{split} is
494 greedily colored, i.e., assigning different time slot–subchannel
495 pairs to interfering virtual links G_{split} , then each link in
496 communication graph $G(V, A)$ certainly satisfies the *link inter-*
497 *ference constraint*. The minimum number of colors (i.e., time
498 slot–subchannel pairs) that G'_{split} consumes is the chromatic
499 number $\chi(G'_{\text{split}})$ [22]. Since W subchannels are available for
500 each time slot, the minimum number of consumed time slots
501 becomes $\lceil (\chi(G'_{\text{split}})/W) \rceil$, when only *link interference con-*
502 *straint* is taken into account. However, in SRORA, there exists
503 the *Tx/Rx constraint*; hence, the optimal number of time slots
504 (i.e., T_{optimal}) must be larger than or equal to $\lceil (\chi(G'_{\text{split}})/W) \rceil$.
505 In other words, $\lceil (\chi(G'_{\text{split}})/W) \rceil \leq T_{\text{optimal}}$ holds.

Second, we derive the upper bound of T_{optimal} by exploring
the property of T_{greedy} . We consider the worst case where
there exists only one subchannel (i.e., $W = 1$). Given any
link assignment order $\vec{\mathcal{L}}$ taken by GR-SRORA, there exists a
corresponding greedy coloring order in G'_{split} . For any greedy
coloring order in G'_{split} , the number of colors that are needed is
at most $\delta(G'_{\text{split}}) + 1$ [23]. Since the number of colors in G'_{split}
is exactly equal to the number of time slots needed in the worst
case communication graph, i.e., $T_{\text{greedy}}^{\text{worst}}(\vec{\mathcal{L}})$, thus, for any link
assignment order $\vec{\mathcal{L}}$, the number of time slots that are consumed
is upper bounded by $T_{\text{max}} = \delta(G'_{\text{split}}) + 1$. In general, the
number of subchannels W is usually a constant greater than 1.
Thus, for any link assignment order $\vec{\mathcal{L}}$, the total number of time
slots needed by GR-SRORA $T_{\text{greedy}}(\vec{\mathcal{L}})$ is equal or smaller than
 $T_{\text{greedy}}^{\text{worst}}(\vec{\mathcal{L}})$. Thus, $T_{\text{greedy}} \leq T_{\text{max}} = \delta(G'_{\text{split}}) + 1$. 520

Combining the lower bound and the upper bound, we have
 $\lceil (\chi(G'_{\text{split}})/W) \rceil \leq T_{\text{optimal}} \leq T_{\text{greedy}} \leq T_{\text{max}} = \delta(G'_{\text{split}}) + 1$,
which proves Theorem 2. \square 523

The complexity of the GR-SRORA is analyzed as follows.
In GR-SRORA, the number of links L is a variable, but sub-
channel number W and traffic demand upper bound M for each
link are constants. In Algorithm 1, lines 2–15 are for assigning
time slots and subchannels to link $l(i, j)$. Its complexity is
 $\mathcal{O}(T_{\text{max}})$, where T_{max} is the upper bound of T_{greedy} . As shown
in Theorem 2, $T_{\text{max}} = \delta(G'_{\text{split}}) + 1$. Since $\delta(G'_{\text{split}}) + 1 \leq$
 $M \times L + 1$, hence, $T_{\text{max}} \leq M \times L + 1$. Thus, the complexity
from lines 2–15 is $\mathcal{O}(L)$. Lines 16–19 are to update $\Phi(i, j, t, s)$
and $\Psi(i, j, t)$. The complexity is $\mathcal{O}(L)$. Thus, considering lines
1–22, the complexity is $L \times (\mathcal{O}(L) + \mathcal{O}(L))$. Therefore, the
total complexity is $\mathcal{O}(L^2)$. 535

C. GA

Since the greedy algorithm, i.e., GR-SRORA, usually can
only obtain the suboptimal solution, we adopt a GA to obtain
a near-optimal result as a theoretical reference for our greedy
algorithm. 540

To apply the GA, the number of decision variables
 $X(i, j, t, s)$ in the optimization problem SRORA needs to be
constant. Since for a certain network the number of links L
and the number of subchannels W are constants, we also need
to fix the total time slots for assignment so that the number
of $X(i, j, t, s)$ will be fixed. From the proof of Theorem 2,
 T_{optimal} is upper bounded by $T_{\text{max}} = \delta(G'_{\text{split}}) + 1$ for a given
communication graph $G(V, A)$. With this bound, the problem
SRORA is reformulated as follows: 549

Minimize T .

$$\text{s.t.} \begin{cases} X(i, j, t, s) + X(p, q, t, s) \leq 1 \\ \left[X(i, j, t, s) + \sum_{f=1}^W \sum_{p \in \text{in}(i)} X(p, i, t, f) \right. \\ \left. + \sum_{g=1}^W \sum_{q \in \text{out}(j)} X(j, q, t, g) \right] \times X(i, j, t, s) \leq 1 \\ \sum_{t=1}^{T_{\text{max}}} \sum_{s=1}^W X(i, j, t, s) \geq D(i, j) \\ X(i, j, t, s) \in \{0, 1\} \\ \forall l(i, j) \in A \quad \forall s = 1, 2, \dots, W \\ \forall l(p, q) \in I_{l(i,j)} \quad \forall t = 1, 2, \dots, T_{\text{max}}. \end{cases}$$

550 The objective T is the maximum occupied time slot in the
 551 network and is calculated with decision variable $X(i, j, t, s)$ as
 552 $T = \max_{t \in \{1, 2, \dots, T_{\max}\}} t$, subject to $\max_{l(i, j) \in A, s \in \{1, 2, \dots, W\}}$
 553 $X(i, j, t, s) \neq 0$. The previous optimization problem is exactly
 554 the same as SRORA, except that the range of t is upper bounded
 555 by T_{\max} instead of T . Thus, its complexity is the same as
 556 SRORA, i.e., it is also NP-complete.

557 Based on this new formulation, a GA is developed for
 558 SRORA. We call it GA-SRORA. Different from classic opti-
 559 mization methods such as gradient-based approaches, GA is
 560 well suited for integer programming problems. Although there
 561 is no absolute guarantee for the GA-SRORA to obtain an
 562 optimal solution, the algorithm can be executed for sufficient
 563 time to reach a near-optimal solution.

564 GA evolves its generation into the next generation via three
 565 essential steps: reproduction, crossover, and mutation. Thus,
 566 GA-SRORA is executed according to the following steps.

- 567 1) Initialize Population: The population of our algorithm
 568 GA-SRORA consists of chromosomes. Each chromo-
 569 some is represented by $X(i, j, t, s)$ of all links.
- 570 2) Evaluation and Fitness Assignment: For every chromo-
 571 some, its fitness needs to be minimized in GA-SRORA.
 572 The fitness captures the objective function and the con-
 573 straints in the reformulated SRORA problem. As a result,
 574 the fitness is described as

Fitness

$$\begin{aligned}
 &= T + P \times (C_1 + C_2 + C_3) \\
 C_1 &= \sum_{l(i, j) \in A} \max \left[0, 1 - \sum_{t=1}^{T_{\max}} \sum_{s=1}^W X(i, j, t, s) / D(i, j) \right] \\
 C_2 &= \sum_{l(i, j) \in A} \sum_{l(p, q) \in I_{l(i, j)}} \sum_{t=1}^{T_{\max}} \sum_{s=1}^W \max \\
 &\quad \times [0, X(i, j, t, s) + X(p, q, t, s) - 1] \\
 C_3 &= \sum_{l(i, j) \in A} \sum_{t=1}^{T_{\max}} \sum_{s=1}^W \max \\
 &\quad \times \left[0, \left(X(i, j, t, s) + \sum_{f=1}^W \sum_{p \in \text{in}(i)} X(p, i, t, f) \right. \right. \\
 &\quad \left. \left. + \sum_{g=1}^W \sum_{q \in \text{out}(j)} X(j, q, t, g) \right) X(i, j, t, s) - 1 \right]
 \end{aligned}$$

575 where T is the maximum occupied time slot in the
 576 network and is obtained with $X(i, j, t, s)$, P as a penalty
 577 parameter. C_1 , C_2 , and C_3 are derived from *traffic de-*
 578 *demand constraint*, *link interference constraint*, and *Tx/Rx*
 579 *constraint*, respectively.

- 580 3) Reproduction: According to the fitness, better chromo-
 581 somes are copied and worse chromosomes are removed,
 582 whereas holding population size constant. A fair selection
 583 is applied to generate “winners” and put them into the
 584 “mating pool.”
- 585 4) Crossover: Parent chromosomes swap a subset of their
 586 strings, generating two new chromosomes called children.

- 587 5) Mutation: A new chromosome is generated by changing
 588 value of one bit in its string. This step reduces the chance
 589 of falling into the local optimal point.
- 590 6) Steps 2–5 are repeated for U rounds to obtain a relatively
 591 stable solution.

The complexity of the GA-SRORA can be derived similarly 592
 to Algorithm 1. For iteration rounds U , population size V , and 593
 link number L , the complexity of GA-SRORA is $\mathcal{O}(UVL^3)$. 594

IV. DISTRIBUTED MEDIUM ACCESS CONTROL FOR 595 ORTHOGONAL FREQUENCY-DIVISION 596 MULTIPLE-ACCESS-BASED CHANNEL-WIDTH 597 ADAPTATION 598

Here, a distributed MAC protocol is designed based on the 599
 greedy algorithm for OFDMA-based channel-width adaptation. 600

A. Distributed Operation of the Greedy Algorithm 601

Four information tables are maintained by every node i : 602
 1) $Q_{\text{in}}(i, p, q)$, which indicates whether subchannel q in time 603
 slot p is occupied by a receiving link (i.e., incoming link) of a 604
 node in the interference range of node i ; 2) $Q_{\text{out}}(i, p, q)$, which 605
 indicates whether subchannel q in time slot p is occupied by a 606
 sending link (i.e., outgoing link) of a node in the interference 607
 range of node i ; 3) $O_{\text{in}}(i, t)$, which indicates whether time slot 608
 t is occupied by any receiving link of node i ; and 4) $O_{\text{out}}(i, t)$, 609
 which indicates whether time slot t is occupied by any sending 610
 link of node i . How such information is collected is explained 611
 in Section IV-C and D. 612

For a given link $l(i, j)$, sending node i is responsible for 613
 assigning time slots and subchannels to support a given number 614
 of units (denoted as $D(i, j)$) in a TDMA frame. With these 615
 variables, resource allocation of link $l(i, j)$ is executed as 616
 follows. 617

- 618 1) Information fusion: Based on the protocol interference 618
 model, any receiving link of a node located in the interfer- 619
 ence range of node i or any sending link of a node located 620
 in the interference range of node j potentially interferes 621
 with link $l(i, j)$; hence, node i needs to communicate with 622
 node j to collect all the resource-allocation information 623
 by combining tables $Q_{\text{in}}(i, p, q)$ and $Q_{\text{out}}(j, p, q)$ before 624
 resource allocation is conducted. Due to the single-radio 625
 OFDMA *Tx/Rx constraint*, node i also needs to obtain 626
 table $O_{\text{out}}(j, t)$ from node j , and then determines which 627
 time slot is still available by checking $O_{\text{in}}(i, t)$ and 628
 $O_{\text{out}}(j, t)$. 629
- 630 2) Time slot and subchannel allocation: For the first time 630
 slot, node i assigns the unoccupied subchannels to link 631
 $l(i, j)$ to support the traffic demands. If the first time slot 632
 is not enough, it goes to the second time slot. This process 633
 is repeated until the sum of the assigned subchannels 634
 can support the traffic demand of link $l(i, j)$. During 635
 this period, any link $l(p, q) \in I_{l(i, j)}$ (i.e., $l(p, q)$ is any 636
 receiving link of a node located in the interference range 637
 of node i or any sending link of a node located in the 638
 interference range of node j) cannot conduct resource 639
 allocation simultaneously. 640

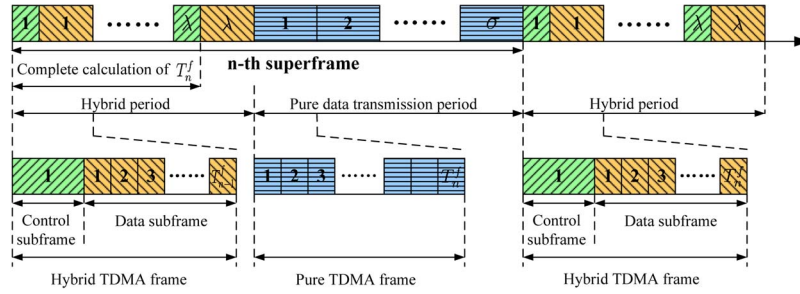


Fig. 3. Frame structure.

3) Information table update: After resource allocation of link $l(i, j)$, all nodes in the interference range of node i and node j update their information tables immediately.

To support the aforementioned mechanisms, the control messages need to be received within the interference range. To this end, the lowest transmission rate is adopted by control messages.

Since every node contends to assign resources to its outgoing links in a greedy way, two nodes that are far away enough can conduct resource allocation simultaneously. As a result, resource allocation in the entire WMN is conducted in a distributed way and is thus called distributed GR-SRORA (DGR-SRORA). Based on this distributed resource-allocation process, a distributed multisubchannel TDMA MAC protocol is developed in the following sections.

B. Frame Structure

The new MAC protocol works in a hybrid way, as shown in Fig. 3. In each superframe, a new resource allocation is carried out in λ control subframes, and data transmissions proceed on the assigned time slots and subchannels.

A superframe includes two parts, namely, hybrid period and pure data transmission period. The hybrid period consists of λ hybrid TDMA frames, where λ is a constant and must be set large enough for all the nodes to complete resource allocation. A hybrid TDMA frame is composed of two subframes: control subframe and data subframe. Each consists of a number of time slots. The control subframe is used for resource allocation. The data subframe is used for data transmission. The pure data transmission period consists of σ pure TDMA frames, where σ is a constant. These TDMA frames are only used for data transmission.

As shown in Fig. 3, in the n th superframe, the length of the data subframe in the hybrid period is T_{n-1}^f , which is determined in the $(n-1)$ -th superframe. In the hybrid period of the n th superframe, our resource-allocation algorithm determines a new length of a TDMA frame T_n^f . This new value updates the length of a pure TDMA frame in the pure data transmission period of the n th superframe. It also determines the length of the data subframe in the hybrid period of the $(n+1)$ -th superframe. As a result, in Fig. 3, the frame lengths in the left hybrid TDMA frame and the right hybrid TDMA frame are equal to T_{n-1}^f and T_n^f , respectively.

In the control subframe of the hybrid period, each node uses an request-to-send/clear-to-send mechanism to contend for time slots' and subchannels' allocation. In all TDMA frames

for data transmission, each node adopts carrier-sense multiple access/collision avoidance to access the assigned time slots and subchannels. This can prevent collisions due to allocation error or out-of-network interference. As a result, our MAC protocol is actually a TDMA MAC overlaying CSMA/CA.

C. Distributed Resource-Allocation Procedure

The control subframe in Fig. 3 is used to signal distributed resource allocation. Control messages are sent with the lowest transmission rate using all subchannels. For resource assignment of link $l(i, j)$, the negotiation between node i and node j follows this procedure.

- 1) Node i sends a request-to-assign (RTA) packet to node j . All nodes except node j in the sensing range of node i keep quiet.
- 2) Upon receiving the RTA packet, node j sends node i a clear-to-assign (CTA) packet, which contains $Q_{out}(j, p, q)$ and $O_{out}(j, t)$. All nodes except node i in the sensing range of node j keep quiet.
- 3) Upon receiving the CTA packet, node i relies on tables $Q_{in}(i, p, q)$, $Q_{out}(j, p, q)$, $O_{in}(i, t)$, and $O_{out}(j, t)$ to assign time slots and subchannels to link $l(i, j)$. Then, node i broadcasts an announcement (ANN) packet, which contains the assignment result for link $l(i, j)$, to all nodes in its interference range.
- 4) Upon receiving the ANN packet, all nodes in the interference range of node i update their tables. Node j also broadcasts an ANN packet to all nodes in its interference range, and then such receiving nodes update their information tables.

An example of resource-allocation procedure is explained next. The signaling messages are transmitted in the lowest rate to cover all the nodes in the interference range, and the exchange procedure is shown in Fig. 4.

- 1) Node A starts to assign time slots and subchannels for link $l(A, B)$. It broadcasts an RTA packet to node B . Node C and node D can receive the signaling packet; hence, they keep quiet.
- 2) Node B receives the RTA packet and then broadcasts a CTA packet, which contains $Q_{out}(B, p, q)$ and $O_{out}(B, t)$, to node A . Nodes A and C can receive this packet, but node D can only sense it.
- 3) Node A receives the CTA packet and broadcasts an ANN packet, which contains the assignment result for link $l(A, B)$. Node B receives this packet, but nodes C and D can only sense it.

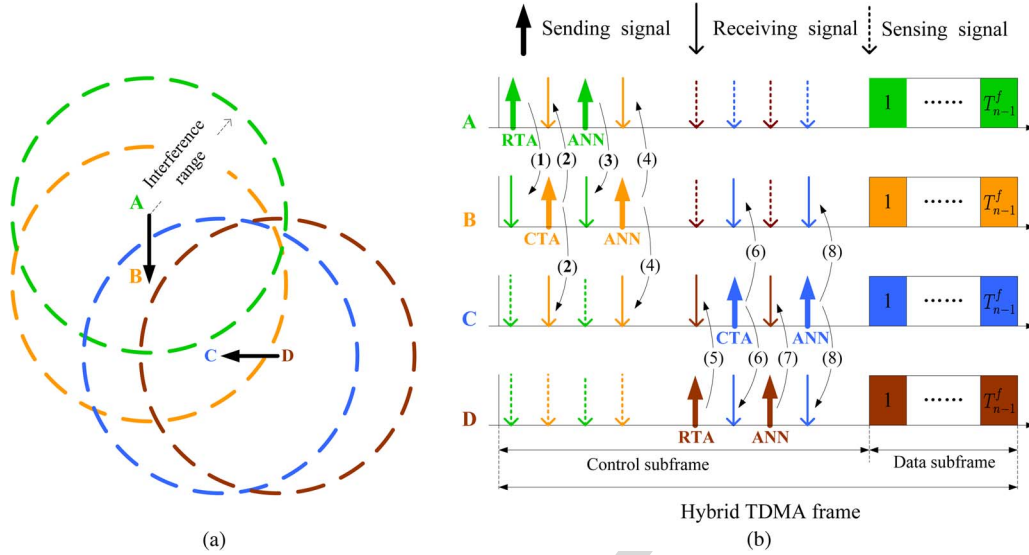


Fig. 4. Operation of the MAC protocol: An example. (a) Topology. (b) Resource negotiation.

- 731 4) When node *B* receives the ANN packet, it updates its
 732 own information tables and rebroadcasts the ANN packet.
 733 Nodes *A* and *C* receive it and update their tables, but node
 734 *D* can only sense it.
- 735 5) Node *D* starts to assign time slots and subchannels for
 736 link $l(D, C)$. It broadcasts an RTA packet to node *C*.
 737 Node *A* and node *B* can sense the signaling; hence, they
 738 keep quiet.
- 739 6) Node *C* receives the RTA packet and then broad-
 740 casts a CTA packet, which contains $Q_{out}(C, p, q)$ and
 741 $O_{out}(C, t)$, to node *D*. Node *D* and node *B* can receive
 742 this packet, but node *A* can only sense it.
- 743 7) Node *D* receives the CTA packet and broadcasts an
 744 ANN packet, which contains the allocation result of link
 745 $l(D, C)$. Node *C* receives this packet, but node *A* and
 746 node *B* can only sense it.
- 747 8) When node *C* receives the ANN packet, it updates its
 748 own information tables and rebroadcasts the ANN packet.
 749 Nodes *D* and *B* receive it and update their information
 750 tables, but node *A* can only sense it.

751 In the distributed algorithm, every node determines its own
 752 time slot. Thus, the largest time slot in one node may be dif-
 753 ferent from that of another node. To avoid inconsistent TDMA
 754 frame in different links, the largest time slot in the allocation
 755 must be known to all nodes. This can be done by the following
 756 simple procedure. When a node gets resource-allocation infor-
 757 mation from another node, it compares its largest time slot with
 758 that in the allocation information. If its own value is smaller,
 759 it needs to update its largest time slot number and broadcast
 760 the updated information to its neighbors; otherwise, no action
 761 is needed.

762 D. Enhancement for Multiple Interference Domains

763 The aforementioned protocol is effective for the single in-
 764 terference domain because every time only one link is in the
 765 resource-allocation process and other nodes can hear signaling
 766 messages and keep quiet. However, in the case of multiple

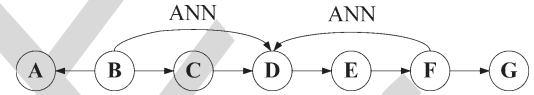


Fig. 5. ANN packet collision may occur in the case of multiple interference domains.

interference domains, there exist collisions in ANN packets. 767
 For example, in Fig. 5, node *B* and node *F* successfully make 768
 reservation for link $l(B, A)$ and link $l(F, G)$ by exchanging 769
 RTA and CTA packets. However, it is possible that the ANN 770
 packets broadcast by node *B* and node *F* simultaneously and 771
 interfere each other at node *D*. Thus, node *D* cannot receive 772
 the ANN packet, which leads to errors in the following resource 773
 assignment in other links. To reduce the probability of colli- 774
 sions in ANN packets, we propose a scheme as follows. During 775
 the resource-allocation process of link $l(i, j)$, node *i* and node 776
j exchange RTA and CTA packets as usual. The process of 777
 broadcasting ANN packets is modified to reduce the collision 778
 probability: 1) Node *i* and node *j* broadcast ANN packets in 779
 turn for K_{ANN} rounds instead of only one round; and 2) be- 780
 fore broadcasting an ANN packet, the sending node randomly 781
 chooses a waiting time in the backoff window W_{ANN} and de- 782
 lays the ANN packet transmission for the chosen waiting time. 783

Although this scheme cannot guarantee collision-free ANN 784
 packets, the collision probability dramatically drops with the 785
 increased K_{ANN} and W_{ANN} . It should be noted that how 786
 to design an effective distributed MAC protocol in multiple 787
 interference domains still remains a challenging problem. 788

789 V. PERFORMANCE RESULTS

790

Here, MATLAB simulations are carried out to evaluate our 790
 algorithms and protocols developed in previous sections. Since 791
 the objective of our algorithms and protocols is to leverage 792
 channel-width adaptation to efficiently support diverse traffic 793
 demands in different links of a WMN, transmission rate in 794
 different links is assumed to be homogeneous. Performance 795
 results from such a setting provide a better demonstration about 796

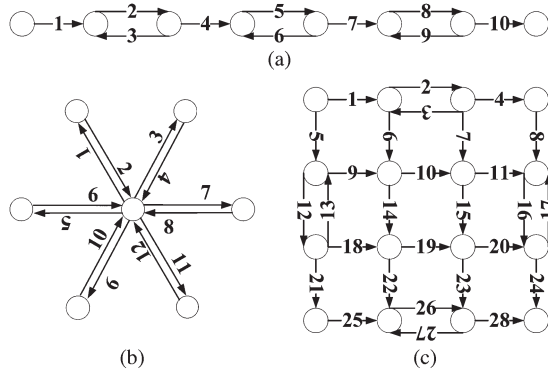


Fig. 6. Simple topologies.

797 how channel-width adaptation improves throughput; the impact
798 from heterogeneous link rates is eliminated. In simulations, the
799 homogeneous link rate is equal to 54 Mb/s when the band-
800 width is 20 MHz. The total available bandwidth is 40 MHz;
801 hence, the corresponding link rate using a whole spectrum
802 is 108 Mb/s. Moreover, a single radio is considered in each
803 mesh node.

804 In our OFDMA-based channel-width adaptation scheme, the
805 whole spectrum is divided into 64 subchannels and the length
806 of a time slot is 5 ms. We assume that one subchannel per time
807 slot can transmit 1 unit of traffic demand. If a link is assigned
808 two subchannels every three time slots, then its throughput
809 is $(2/3) \times (108/64) = 1.125$ Mb/s. The network throughput is
810 defined as the ratio of the total supported traffic demands over
811 the length of a TDMA frame.

812 To fully evaluate our algorithm and protocols, different net-
813 work topologies are considered in the following sections. The
814 details of network setup and the corresponding traffic demands
815 are specified separately for each topology.

816 A. Simple Topologies

817 The greedy algorithm and GA are evaluated under three
818 simple topologies in Fig. 6. In each topology, the link ID is
819 marked in the figure, and all the links have the same length,
820 which represents the communication range. The interference
821 range is set twice the communication range.

822 For each link, the traffic demand is uniformly distributed in
823 $\{1, \dots, 128\}$ (units).

824 For each topology, we evaluate the network throughput
825 that can be achieved in a WMN with available bandwidth
826 of 40 MHz. The performance results of our channel-width
827 adaptation algorithms (i.e., GR-SRORA and GA-SRORA) are
828 compared with that achieved by the single-radio traditional
829 channel-width adaptation (SRTCWA) scheme and also with
830 that achieved by the single-radio fixed channel-width (SRFCW)
831 scheme. SRTCWA and SRFCW are executed following the
832 same procedure as GR-SRORA (i.e., greedily assign time slot
833 and channel to all the links in the same order as GR-SRORA)
834 but consider different constraints. In SRTCWA, there are four
835 options of channel width (i.e., 5, 10, 20, and 40 MHz), and the
836 center frequency of each channel can be adjusted. In SRFCW,
837 the radio on each node uses a 20-MHz channel. To be fair in
838 comparison, two orthogonal channels (i.e., totally 40 MHz) are

available in SRFCW for parallel links in the same interference
839 domain. 840

In the string topology, as shown in Fig. 7(a), on average, the
841 network throughput of GR-SRORA is 19.2% higher than that
842 achieved by SRTCWA and 30.8% higher than that of SRFCW.
843 In this network structure, the throughput improvement is not
844 significant due to lack of PMP structure in the string topology.
845

In the star topology, as shown in Fig. 7(b), on average,
846 the network throughput of GR-SRORA is 54.5% higher than
847 that of SRTCWA and 136.4% higher than that of SRFCW.
848 The improvement is significant because our OFDMA-based
849 channel-width adaptation scheme is very suitable for explor-
850 ing channel-width adaptive concurrent transmissions in a star
851 network structure. 852

In the grid topology, as shown in Fig. 7(c), on average, the
853 network throughput of GR-SRORA is 19.3% higher than that
854 of SRTCWA and 29.8% higher than that of SRFCW. 855

As shown in Fig. 7, the greedy algorithm achieves nearly
856 the same throughput as that of the GA-based algorithm, which
857 indicates that the greedy algorithm is effective to obtain a
858 near-optimal solution to the channel-width adaptation problem
859 in WMNs. 860

B. Randomized Topology 861

Our distributed MAC protocol is also evaluated in a ran-
862 domized topology. The communication range of each node is
863 100 m, the interference range is 200 m, and the sensing range is
864 300 m. The RTA and CTA packets have a length of 120 bytes,
865 and the ANN packet has a length of 30 bytes. As explained in
866 Section IV, the lowest transmission rate is adopted to send these
867 packets, and it is set to 6 Mb/s. 868

1) *Single Interference Domain Scenario*: In this scenario,
869 nodes are randomly distributed within a circle with a diameter
870 of 200 m. Since all nodes can hear each other, no collision is
871 associated with ANN packets. The distributed MAC protocol
872 (DGR-SRORA) in Section IV is adopted. The ANN packets
873 are broadcast only for one round. In the simulation, six cases
874 of node-link pairs are considered: 10 nodes 15 links, 10 nodes
875 20 links, 20 nodes 30 links, 20 nodes 40 links, 30 nodes 45
876 links, and 30 nodes 60 links. For each case, the nodes are
877 randomly distributed and the links are randomly selected. The
878 traffic demand for each link is uniformly distributed within
879 $\{1, \dots, 128\}$ (units). 880

a) *Network throughput*: In each case of node-link pair,
881 the distributed protocol DGR-SRORA is compared with
882 SRTCWA and SRFCW. The network throughput of each case
883 is averaged over five tests and is shown in Fig. 8. In all
884 cases, our OFDMA-based channel-width adaptation scheme
885 outperforms SRTCWA and SRFCW. Moreover, compared with
886 the SRTCWA, DGR-SRORA improves the network throughput
887 by 14.3%, 20.0%, 18.5%, 15.0%, 13.3%, and 16.1%, respec-
888 tively, in six cases. As compared with SRFCW, DGR-SRORA
889 enhances the network throughput by 28.6%, 30.0%, 29.6%,
890 25.0%, 22.2%, and 24.2%, respectively, in six cases. 891

b) *Resource-allocation delay*: The total time required for
892 the distributed resource-allocation procedure is investigated. In
893 our simulation, the sum of the control subframe and the data
894

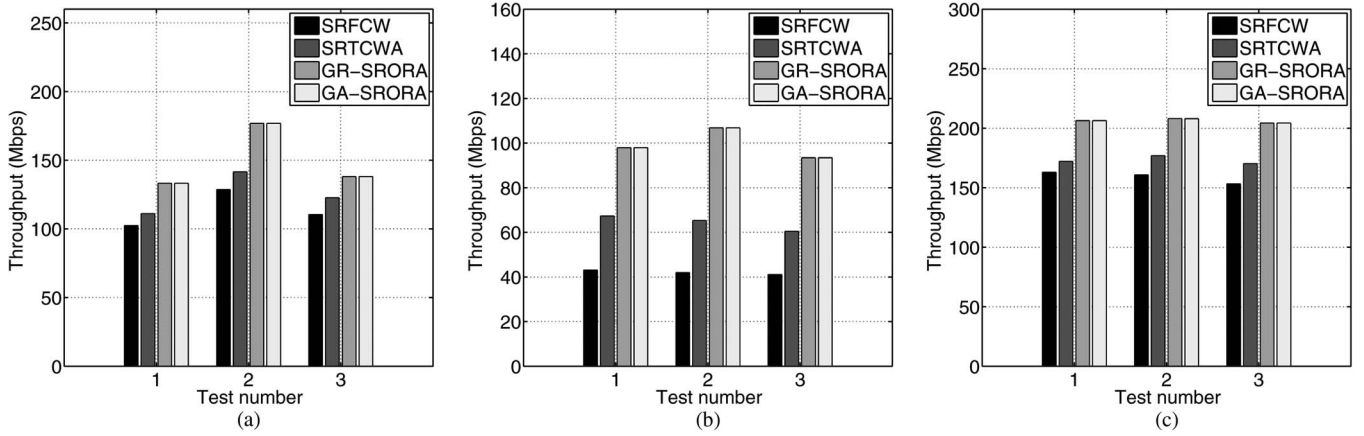


Fig. 7. Network throughput for simple topologies. (a) String topology. (b) Star topology. (c) Grid topology.

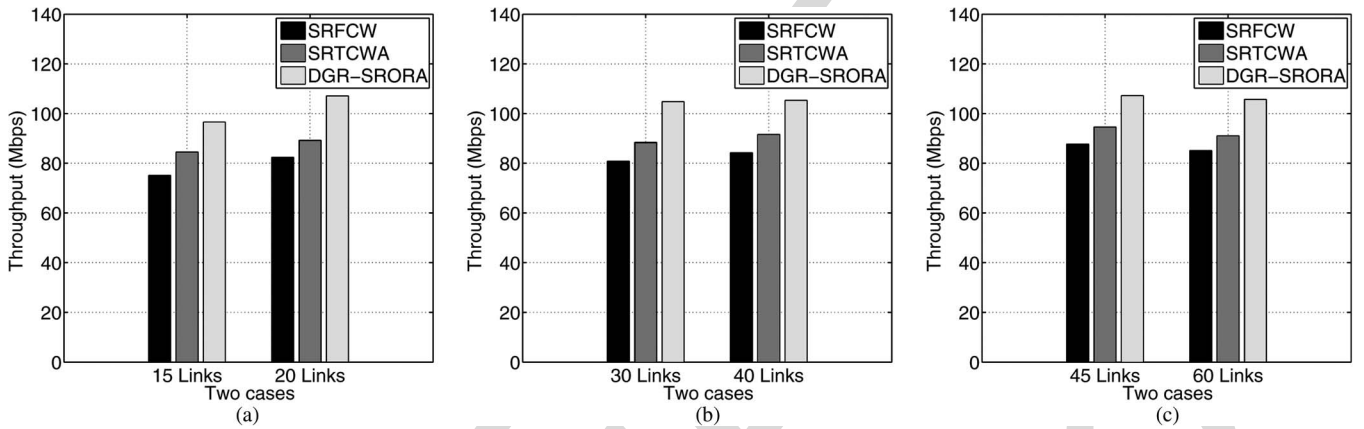


Fig. 8. Network throughput in the scenario of single interference domain. (a) 10 nodes. (b) 20 nodes. (c) 30 nodes.

TABLE I
TOTAL RESOURCE ALLOCATION TIME FOR THE SINGLE INTERFERENCE DOMAIN SCENARIO

Control Subframe	Data Subframe	Nodes: 10 Links: 15	Nodes: 10 Links: 20	Nodes: 20 Links: 30	Nodes: 20 Links: 40	Nodes: 30 Links: 45	Nodes: 30 Links: 60
20 ms	80 ms	9.2 ms	11.3 ms	18.4 ms	104.5 ms	112.1 ms	202.3 ms
15 ms	85 ms	9.2 ms	11.3 ms	103.9 ms	110.5 ms	202.4 ms	214.7 ms
10 ms	90 ms	9.2 ms	101.8 ms	200.5 ms	205.9 ms	305.7 ms	407.0 ms
5 ms	95 ms	104.0 ms	202.5 ms	304.7 ms	504.4 ms	801.5 ms	1100.5 ms

895 subframe (i.e., the length of a hybrid TDMA frame) is assumed 896 to be 100 ms. For each case of node-link pair, we consider 897 different lengths of control subframe and data subframe. The 898 results are shown in Table I. For each case of node-link pair, 899 when the control subframe is longer, the allocation delay is 900 smaller. Thus, if we need a faster allocation procedure, a larger 901 control subframe is necessary, which leads to more overhead in 902 signaling. However, even if the overhead is less than 10% for 903 signaling, the allocation can be done within 1 s for node-link 904 pairs: 10–15, 10–20, 20–30, 20–40, and 30–45. Such a fast 905 allocation procedure means that our MAC protocol is highly 906 adaptive to dynamic network conditions such as topology 907 change or traffic variations.

908 *Scenario of Multiple Interference Domains:* In this scenario, 909 50 nodes are randomly distributed in a square whose side 910 length is 1000 m, as shown in Fig. 9. The distributed MAC 911 protocol with modified ANN packet transmission in Section IV

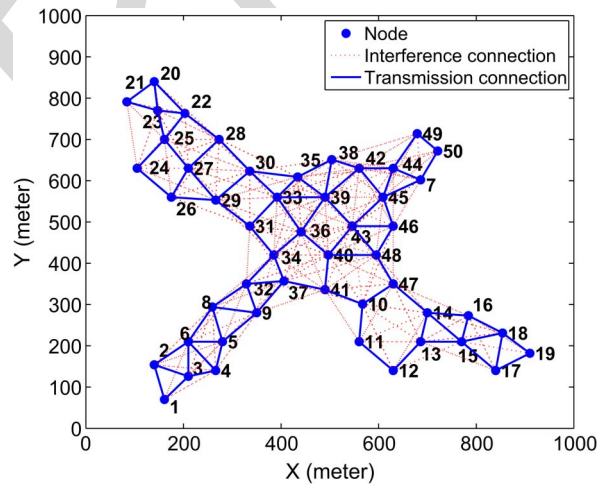


Fig. 9. Topology.

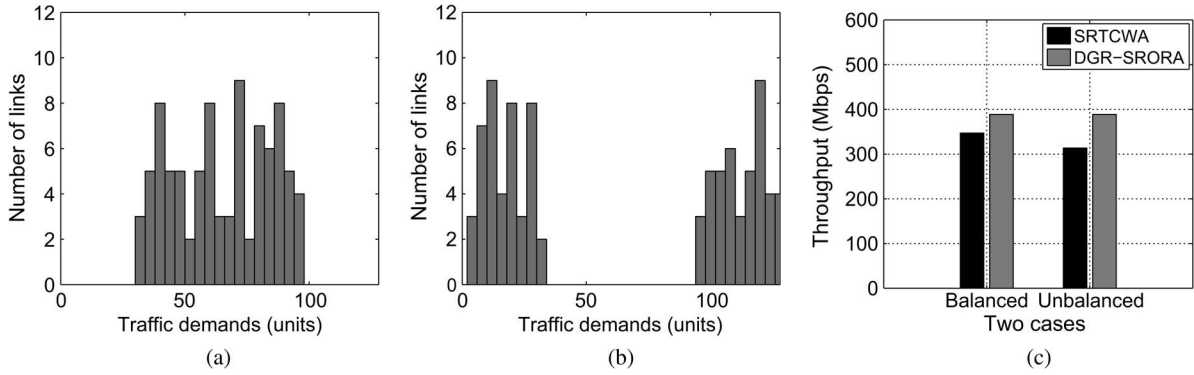


Fig. 10. Network throughput under different traffic distributions. (a) Balanced traffic distribution. (b) Unbalanced traffic distribution. (c) Network throughput.

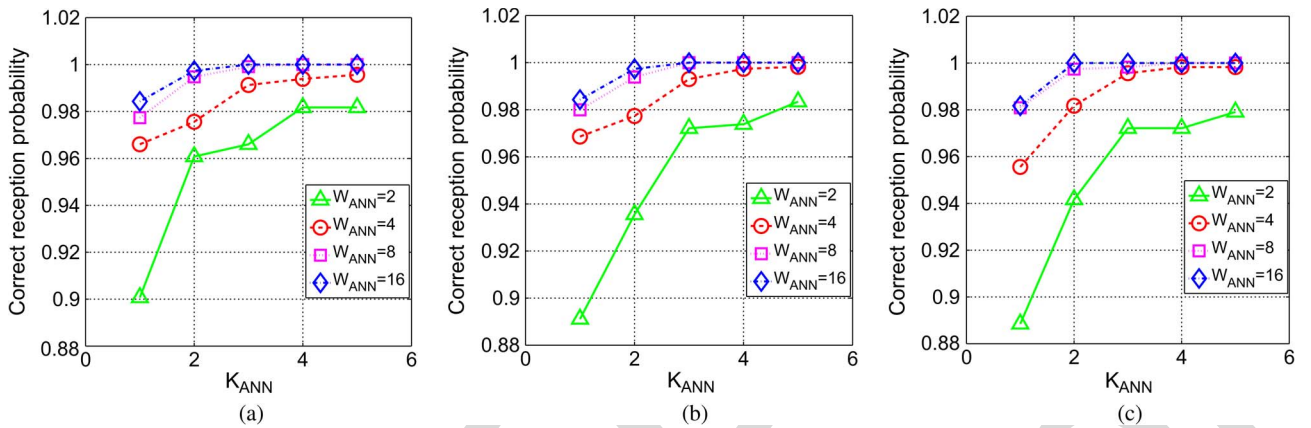


Fig. 11. ANN packet reception probability in the network with multiple interference domains. (a) Control subframe: 10 ms. (b) Control subframe: 15 ms. (c) Control subframe: 20 ms.

912 is adopted. In this protocol, the ANN packets are broadcast after 913 a randomly chosen waiting time for several rounds.

914 *c) Network throughput:* The impact of the traffic dis- 915 tribution to the network throughput is illustrated in Fig. 9. 916 Since there exists multiple interference domains, the distributed 917 protocol DGR-SRORSA may have allocation error due to col- 918 lision in ANN packets. Thus, we properly choose broadcasting 919 rounds and backoff window to reduce collisions. We randomly 920 choose 88 links in Fig. 9 for the test. Two cases with different 921 traffic distributions are considered. In the first case, the traffic 922 demand of each link is balanced and is uniformly distributed 923 in $\{32, \dots, 96\}$, as shown in Fig. 10(a). In the second case, 924 the traffic demand of each link is unbalanced and is uni- 925 formly distributed in either $\{1, 32\}$ or $\{96, 128\}$, as shown 926 in Fig. 10(b). The network throughputs of these two cases are 927 shown in Fig. 10(c). As compared with the traditional channel- 928 width adaptation scheme (i.e., SRTCWA), our MAC protocol 929 with OFDMA-based channel-width adaptation improves the 930 network throughput by 12% and 24%, respectively, in these two 931 cases. Higher throughput improvement is achieved in the case 932 of unbalanced traffic distribution because our MAC protocol 933 leverages OFDMA-based channel-width adaptation to allocate 934 resource in more proper way.

935 *d) Performance of the modified ANN packet broadcasting 936 mechanism:* In Section IV-D, we propose that an ANN packet

is broadcast after a randomly selected waiting time for several 937 rounds to reduce the collision probability. In this experiment, 938 this mechanism is investigated with respect to different broad- 939 casting rounds K_{ANN} and backoff window W_{ANN} . In Fig. 9, 940 we randomly choose 88 links for testing. Three cases (with 10-, 941 15-, and 20-ms control subframes) are considered. In each 942 case, the number of broadcasting rounds K_{ANN} varies from 943 1 to 5, and the broadcasting delay is randomly chosen in the 944 backoff window W_{ANN} . W_{ANN} is set 2, 4, 8, and 16 (the unit 945 is the transmission time of an ANN packet), respectively. The 946 reception probability of ANN packets is defined as the ratio 947 of the correctly received ANN packets over total transmitted 948 ANN packets. In Fig. 11, for the fixed K_{ANN} in all cases, 949 the correct reception probability is higher with larger W_{ANN} . 950 Similarly, for the fixed W_{ANN} , the correct reception probability 951 increases with a larger K_{ANN} . In each case, when $K_{ANN} = 952$ 3 and $W_{ANN} = 16$ or when $K_{ANN} = 4$ and $W_{ANN} = 8$, the 953 reception probability near reaches 1. 954

e) Resource-allocation delay: The total delay required 955 for the distributed resource-allocation procedure is also inves- 956 tigated. In our simulation, the sum of the control subframe and 957 the data subframe is assumed to be 100 ms, and three cases 958 (with 10-, 15-, and 20-ms control subframes) are considered. 959 The results are shown in Table II. When the control subframe is 960 longer, the allocation delay is smaller. Thus, if we need a faster 961

TABLE II
TOTAL RESOURCE ALLOCATION DELAY FOR THE SCENARIO OF MULTIPLE INTERFERENCE DOMAINS

Rounds	$W_{ANN}(10ms)^a$				$W_{ANN}(15ms)^b$				$W_{ANN}(20ms)^c$			
	2	4	8	16	2	4	8	16	2	4	8	16
$K_{ANN}=1$	0.20s	0.31s	0.50s	1.01s	0.11s	0.20s	0.31s	0.51s	0.10s	0.11s	0.21s	0.41s
$K_{ANN}=2$	0.21s	0.40s	0.71s	1.21s	0.20s	0.21s	0.41s	0.81s	0.11s	0.20s	0.31s	0.52s
$K_{ANN}=3$	0.31s	0.50s	0.91s	1.70s	0.20s	0.30s	0.51s	1.11s	0.12s	0.21s	0.40s	0.71s
$K_{ANN}=4$	0.40s	0.60s	1.21s	2.70s	0.21s	0.40s	0.61s	1.51s	0.20s	0.30s	0.51s	0.90s
$K_{ANN}=5$	0.50s	0.70s	1.31s	3.30s	0.30s	0.41s	0.80s	1.70s	0.21s	0.31s	0.52s	1.10s

^aThe length of the control subframe is 10 ms

^bThe length of the control subframe is 15 ms

^cThe length of the control subframe is 20 ms

962 allocation procedure, a larger control subframe is necessary,
963 which leads to more overhead in signaling. In each case, for
964 a fixed K_{ANN} , the allocation delay becomes larger as W_{ANN}
965 increases. Similarly, for a fixed W_{ANN} , the allocation delay
966 grows as K_{ANN} increases. For $K_{ANN} = 3$ and $W_{ANN} = 16$,
967 the maximum resource-allocation delay among three cases is
968 1.70 s (i.e., in the 10 ms control subframe case). For $K_{ANN} =$
969 4 and $W_{ANN} = 8$, the maximum resource-allocation delay
970 among three cases is 1.21 s (i.e., in the 10 ms control subframe
971 case). Therefore, with 10% signaling overhead (due to the
972 control subframe), the reception probability reaches 1 with a
973 resource-allocation delay of less than 2 s.

974

VI. CONCLUSION

975 In WMNs, there always exists a mismatch between link
976 capacity and traffic demand. In this paper, an OFDMA-based
977 channel-width adaptation mechanism has been designed to
978 alleviate such a mismatch of each link in WMNs. It was
979 formulated as a time slot and subchannel allocation problem
980 and was proved to be NP-complete. Thus, a greedy algorithm
981 and a GA were derived to obtain a suboptimal solution. Based
982 on the greedy algorithm, a distributed MAC protocol was de-
983 veloped to conduct channel-width adaptation for all links in the
984 WMN. Simulation results showed that the new MAC protocol
985 outperformed MAC protocols with traditional channel-width
986 adaptation. The channel-width adaptation mechanism studied
987 in this paper assumes that the traffic demand on each link is
988 given. In practice, traffic demand of a link is closely related
989 to MAC/routing cross-layer design. How to consider channel-
990 width adaptation under the framework of MAC/routing cross-
991 layer design is a key factor to further improve the network
992 performance of WMNs, which is an interesting topic for future
993 research.

994

REFERENCES

995 [1] R. Chandra, R. Mahajan, T. Moscibroda, R. Raghavendra, and P. Bahl, "A
996 case for adapting channel width in wireless networks," *ACM SIGCOMM*
997 *Comput. Commun. Rev.*, vol. 38, no. 4, pp. 135–146, 2008.
998 [2] L. Cheng, B. Henty, R. Cooper, D. Stancil, and F. Bai, "A measure-
999 ment study of time-scaled 802.11 a waveforms over the mobile-to-mobile
1000 vehicular channel at 5.9 GHz," *IEEE Commun. Mag.*, vol. 46, no. 5,
1001 pp. 84–91, May 2008.
1002 [3] T. Moscibroda, R. Chandra, Y. Wu, S. Sengupta, P. Bahl, and Y. Yuan,
1003 "Load-aware spectrum distribution in wireless LANs," in *Proc. IEEE*
1004 *ICNP*, 2008, pp. 137–146.

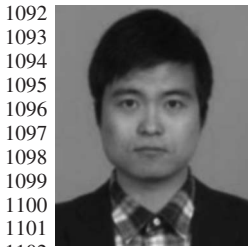
[4] P. Bahl, R. Chandra, T. Moscibroda, S. Narlanka, Y. Wu, and Y. Yuan, 1005
"Dynamic channel-width allocation in wireless networks," U.S. Patent 1006
8243 612, Aug. 14, 2012. 1007
[5] Y. Azar, A. Madry, T. Moscibroda, D. Panigrahi, and A. Srinivasan, 1008
"Maximum bipartite flow in networks with adaptive channel width," 1009
Theoretical Comput. Sci., vol. 412, no. 24, pp. 2577–2587, 1010
May 2011. 1011
[6] I. Akyildiz, X. Wang, and W. Wang, "Wireless mesh networks: A survey," 1012
Comput. Netw., vol. 47, no. 4, pp. 445–487, Mar. 2005. 1013
[7] D. Bharadia, E. McMillin, and S. Katti, "Full duplex radios," *Proc. ACM* 1014
SIGCOMM, pp. 375–386, 2013. 1015
[8] J. So and N. Vaidya, "Multi-channel MAC for ad hoc networks: Handling 1016
multi-channel hidden terminals using a single transceiver," in *Proc. 5th* 1017
ACM Int. Symp. MobiHoc, 2004, pp. 222–233. 1018
[9] R. Maheshwari, H. Gupta, and S. Das, "Multichannel MAC proto- 1019
cols for wireless networks," in *Proc. IEEE SECON*, 2006, vol. 2, 1020
pp. 393–401. 1021
[10] E. Aryafar, O. Gurewitz, and E. Knightly, "Distance-1 constrained chan- 1022
nel assignment in single radio wireless mesh networks," in *Proc. IEEE* 1023
Conf. INFOCOM, 2008, pp. 762–770. 1024
[11] A. Das, H. Alazemi, R. Vijayakumar, and S. Roy, "Optimization models 1025
for fixed channel assignment in wireless mesh networks with multiple 1026
radios," in *Proc. IEEE SECON*, 2005, pp. 463–474. 1027
[12] A. Subramanian, H. Gupta, S. Das, and J. Cao, "Minimum interference 1028
channel assignment in multiradio wireless mesh networks," *IEEE Trans.* 1029
Mobile Comput., vol. 7, no. 12, pp. 1459–1473, Dec. 2008. 1030
[13] X. Li, A. Nusairat, Y. Wu, Y. Qi, J. Zhao, X. Chu, and Y. Liu, 1031
"Joint throughput optimization for wireless mesh networks," *IEEE Trans.* 1032
Mobile Comput., vol. 8, no. 7, pp. 895–909, Jul. 2009. 1033
[14] K. Lee and V. Leung, "Fair allocation of subcarrier and power in an 1034
OFDMA wireless mesh network," *IEEE J. Sel. Areas Commun.*, vol. 24, 1035
no. 11, pp. 2051–2060, Nov. 2006. 1036
[15] H. Cheng and W. Zhuang, "Novel packet-level resource allocation with 1037
effective QoS provisioning for wireless mesh networks," *IEEE Trans.* 1038
Wireless Commun., vol. 8, no. 2, pp. 694–700, Feb. 2009. 1039
[16] A. Bayan and T. Wan, "A scalable QoS scheduling architecture for 1040
WiMAX multi-hop relay networks," in *Proc. 2nd ICETC*, 2010, vol. 5, 1041
pp. V5-326–V5-331. 1042
[17] S. Bai, W. Zhang, Y. Liu, and C. Wang, "Max–min fair scheduling in 1043
OFDMA-based multi-hop WiMAX mesh networks," in *Proc. IEEE ICC*, 1044
2011, pp. 1–5. 1045
[18] Y. Mai and K. Chen, "Design of zone-based bandwidth management 1046
scheme in IEEE 802.16 multi-hop relay networks," *EURASIP J. Wireless* 1047
Commun. Netw., no. 1, pp. 1–28, 2011. 1048
[19] S. Kim, X. Wang, and M. Madhian, "Optimal resource alloca- 1049
tion in multi-hop OFDMA wireless networks with cooperative relay," 1050
IEEE Trans. Wireless Commun., vol. 7, no. 5, pp. 1833–1838, 1051
May 2008. 1052
[20] K. Jain, J. Padhye, V. Padmanabhan, and L. Qiu, "Impact of interference 1053
on multi-hop wireless network performance," *Wireless Netw.*, vol. 11, 1054
no. 4, pp. 471–487, Jul. 2005. 1055
[21] M. Garey and D. Johnson, *Computers and Intractability: A Guide to* 1056
the Theory of NP-Completeness. San Francisco, CA, USA: Freeman, 1057
1979. 1058
[22] J. Bondy and U. Murty, *Graph Theory With Applications*. London, U.K.: 1059
MacMillan, 1976. 1060
[23] D. Johnson, "Worst case behavior of graph coloring algorithms," in *Proc.* 1061
5th Southeastern Conf. Combinatorics, Graph Theory Comput., 1974, 1062
pp. 513–527. 1063



Xudong Wang (SM'08) received the Ph.D. degree in electrical and computer engineering from Georgia Institute of Technology, Atlanta, GA, USA, in 2003.

He has been with several companies as a Senior Research Engineer, a Senior Network Architect, and an R&D Manager. He is currently with the University of Michigan-Shanghai Jiao Tong University (UM-SJTU) Joint Institute, Shanghai Jiao Tong University, Shanghai, China. He is a Distinguished Professor (Shanghai Oriental Scholar) and is the Director of the Wireless And Networking (WANG) Laboratory. He is also an affiliate faculty member with the Department of Electrical Engineering, University of Washington, Seattle, WA, USA. He has been actively involved in R&D, technology transfer, and commercialization of various wireless networking technologies. He holds several patents on wireless networking technologies, and most of his inventions have been successfully transferred to products. His research interests include wireless communication networks, smart grid, and cyber physical systems.

Dr. Wang was a voting member of the IEEE 802.11 and 802.15 Standards Committees. He is an Editor of the IEEE TRANSACTIONS ON VEHICULAR TECHNOLOGY, Elsevier's *Ad Hoc Networks*, and ACM/Kluwer's *Wireless Networks*. He has been a Guest Editor of several journals. He was the demo Co-Chair of the ACM International Symposium on Mobile Ad Hoc Networking and Computing (ACM MOBIHOC 2006), a Technical Program Co-chair of 2008 the Wireless Internet Conference (WICON) 2007, and a General Co-chair 2009 of WICON 2008. He has been a Technical Committee Member of many international conferences and a Technical Reviewer for numerous international journals and conferences.



Pengfei Huang received the B.E. degree in electrical engineering from Zhejiang University, Hangzhou, China, in 2010 and the M.S. degree in electrical engineering from Shanghai Jiao Tong University, Shanghai, China, in 2013. He is currently working toward the Ph.D. degree with the Department of Electrical and Computer Engineering, University of California at San Diego, La Jolla, CA, USA.

His current research interests are in the area of wireless communications and networking, with an emphasis on the design and performance analysis of real-time video transmission over wireless channel.



Jiang (Linda) Xie (SM'09) received the B.E. degree from Tsinghua University, Beijing, China, in 1997; the M.Phil. degree from The Hong Kong University of Science and Technology, Kowloon, Hong Kong, in 1999; and the M.S. and Ph.D. degrees from the Georgia Institute of Technology, Atlanta, GA, USA, in 2002 and 2004, respectively, all in electrical and computer engineering.

In August 2004, she joined the Department of Electrical and Computer Engineering, University of North Carolina, Charlotte (UNC-Charlotte), NC, USA, as an Assistant Professor. Currently, she is an Associate Professor. Her current research interests include resource and mobility management in wireless networks, quality-of-service provisioning, and next-generation Internet.

Dr. Xie is a Senior Member of the Association for Computing Machinery (ACM). She serves on the editorial boards of the IEEE TRANSACTIONS ON MOBILE COMPUTING, *IEEE Communications Surveys and Tutorial*, *Computer Networks* (Elsevier), the *Journal of Network and Computer Applications* (Elsevier), and the *Journal of Communications* (ETPub). She received the U.S. National Science Foundation Faculty Early Career Development (CAREER) Award in 2010, a Best Paper Award from the IEEE/Web Intelligence Congress/ACM International Conference on Intelligent Agent Technology (IAT 2010), and a Graduate Teaching Excellence Award from the College of Engineering from UNC-Charlotte in 2007.



Mian Li received the B.E. and M.S. degrees from Tsinghua University, Beijing, China, in 1994 and 2001, respectively, and the Ph.D. degree from the University of Maryland, College Park, MD, USA, in 2007 with the Best Dissertation Award.

Currently, he is a tenure-track Assistant Professor with the University of Michigan-Shanghai Jiao Tong University (UM-SJTU) Joint Institute, Shanghai Jiao Tong University, Shanghai, China. Within the Mechanical Engineering Program at UM-SJTU Joint Institute, his research work has been focused on robust/reliability-based multidisciplinary design optimization and sensitivity analysis, including topics such as multidisciplinary design optimization, robust/reliability design, sensitivity analysis, and approximation modeling.

AUTHOR QUERIES

AUTHOR PLEASE ANSWER ALL QUERIES

AQ1 = Please check if change made in this sentence is appropriate.

AQ2 = Semi-colon was changed to comma. Please check if appropriate.

AQ3 = The preceding statement is incomplete. Hence, it was combined with the subsequent sentence. Please check if appropriate.

END OF ALL QUERIES

IEEE
Proof

OFDMA-Based Channel-Width Adaptation in Wireless Mesh Networks

Xudong Wang, *Senior Member, IEEE*, Pengfei Huang, Jiang Xie, *Senior Member, IEEE*, and Mian Li

Abstract—Channel-width adaptation can optimize multiple performance metrics of a wireless communication link, including transmission rate, communication range, resilience to delay spread, and power consumption. Supporting variable channel width has been considered one of the most critical features of a communication radio. How to leverage a channel-width adaptive radio to improve throughput of a wireless network is a challenging problem in the medium access control (MAC) layer. So far, there exist research results on either theoretical analysis or protocol implementation for a point-to-multipoint (PMP) infrastructure network. However, the impact of channel width to a multihop wireless network has not been fully investigated yet. More specifically, how to exploit variable channel width to enhance throughput of a multihop wireless network remains an unresolved research issue. This paper addresses this issue in wireless mesh networks (WMNs) considering orthogonal frequency-division multiple-access (OFDMA)-based channel-width adaptation. Theoretical analysis is first carried out to identify appropriate algorithms for channel width adaptation. To this end, resource allocation with OFDMA-based channel-width adaptation is formulated as an optimization problem, which is proved to be NP-complete. To reduce the computational complexity, a greedy algorithm is derived to obtain a suboptimal solution. Based on such a greedy algorithm, a distributed MAC protocol is designed for channel-width adaptation for OFDMA-based WMNs. It takes advantage of variable channel width in different time slots to achieve highly efficient resource allocation. Simulation results illustrate that the distributed MAC protocol significantly outperforms MAC protocols based on traditional channel-width adaptation.

Index Terms—Channel-width adaptation, distributed medium access control (MAC) protocol, wireless mesh networks (WMNs).

I. INTRODUCTION

ADJUSTING channel width can optimize a few performance metrics of a wireless communication link. For example, given a certain level of transmission power, reducing the channel width of a wireless link can reliably increase its communication range; if the channel width is further reduced,

then the power consumption can be also decreased without compromising the communication range. Thus, channel-width adaptation can optimize both communication range and power consumption that are usually in conflict with each other in a wireless link with fixed channel width [1]. Considering another scenario where a vehicular network is built based on orthogonal frequency-division multiplexing (OFDM), when a vehicle moves from a rural area to a suburb area, the delay spread of its communication link may increase to a level larger than the guard interval of OFDM symbols; however, reducing channel width is effective to fix this problem [2].

Because of the benefits of channel-width adaptation, supporting multiple options of channel width in a communication radio has become a common practice. For example, many IEEE 802.11 chipsets made by Atheros (now part of Qualcomm) support channel widths of 5, 10, 20, and 40 MHz. Similarly, WiMAX and long-term evolution chipsets also support a set of different channel widths. However, how to utilize such communication radios to improve network performance is a nontrivial task because a wireless network usually involves many communication links that all demand channel-width adaptation. In a point-to-multipoint (PMP) wireless network such as the IEEE 802.11 basic service set in infrastructure mode or an extended PMP network such as the IEEE 802.11 extended service set, research work has been conducted to utilize channel-width adaptation. In [1], the advantages of channel-width adaptation are analyzed using commodity IEEE 802.11 radios. A simple channel-width adaptation algorithm is derived for the basic scenario of a single link with two communication nodes. In [3] and [4], the channel widths of all access points in the distribution system of an IEEE 802.11 network are optimized according to different traffic load distributions in each basic service set. As a result, the throughput and the fairness of bandwidth distribution of the entire IEEE 802.11 network are greatly enhanced [3], [4]. A general case of adaptive channel-width allocation in base stations considering the demands of clients is analyzed in [5], where throughput maximization is formulated as a maximum bipartite flow problem.

The channel-adaptation algorithms in [1] and [3]–[5] are not applicable to a multihop wireless network because they all assume that the network works in a single-hop infrastructure mode. For multihop wireless networks, there still lack channel-width adaptation algorithms. Different types of multihop wireless networks are characterized by different features, which leads to different requirements and challenges in channel-width adaptation. For example, in a mobile ad hoc network, channel-width adaptation can be utilized to compensate delay spread and increase link stability. However, since the network

Manuscript received August 3, 2013; revised November 23, 2013; accepted February 1, 2014. This work was supported in part by the National Natural Science Foundation of China under Grant 61172066, by the Oriental Scholar Program of Shanghai Municipal Education Commission, and by Shanghai Pujiang Scholar Program 10PJ1406100. The review of this paper was coordinated by Prof. Y. Qian.

X. Wang and M. Li are with the University of Michigan-Shanghai Jiao Tong University (UM-SJTU) Joint Institute, Shanghai Jiao Tong University, Shanghai 200240, China (e-mail: wxudong@ieee.org).

P. Huang is with the Department of Electrical and Computer Engineering, University of California at San Diego, La Jolla, CA 92093, USA.

J. Xie is with the University of North Carolina, Charlotte, NC 28223 USA.

Color versions of one or more of the figures in this paper are available online at <http://ieeexplore.ieee.org>.

Digital Object Identifier 10.1109/TVT.2014.2308316

89 topology is highly variable due to mobility, allocating different
 90 channel widths to different links is an extremely challenging
 91 task. In a wireless mesh network (WMN) [6], mobility is
 92 minimal. In particular, in the infrastructure of a WMN, all
 93 communication links remain stationary [6]. As a result, issues
 94 such as communication range, delay spread, and link stability
 95 can be considered during the network design and deployment
 96 phase. However, there exists one highly variable parameter
 97 that impacts the performance of WMNs, which is traffic load
 98 distribution on each link. It is rather common in WMNs that
 99 some links experience heavy traffic, whereas other links support
 100 only light traffic. To conduct efficient resource allocation for
 101 these links, a link with light traffic must be assigned with a very
 102 small resource unit, whereas a link with heavy traffic needs a
 103 large number of such resource units. If a time slot with fixed
 104 channel width is considered as a resource unit, then it is difficult
 105 to achieve the fine granularity of a small resource unit. For
 106 example, in many wireless networks, a link with fixed channel
 107 width can deliver a rate of 50 Mb/s or more; to achieve a
 108 resource unit of 100 Kb/s, the time slot length is 240 μ s when
 109 the frame size is 1500 bytes and can be as small as 24 μ s when
 110 the frame size is 150 bytes. Implementing such a small time slot
 111 is extremely challenging and can also result in large overhead
 112 due to the need of guard time. This problem can be properly
 113 solved by leveraging channel-width adaptation. More specifi-
 114 cally, a fine-grained resource unit can be achieved by reducing
 115 channel width in a time slot. Thus, in this paper, channel-width
 116 adaptation algorithms and protocols are developed to satisfy
 117 heterogeneous traffic demands on various links in WMNs.

118 Traditionally, channel width of a link can be adjusted by se-
 119 lecting different options (e.g., 5, 10, 20, and 40 MHz) available
 120 in a radio. To consider finer channel-width adaptation, orthogo-
 121 nal frequency-division multiple-access (OFDMA) is adopted.
 122 We consider a single-radio WMN, where each radio adopts
 123 OFDMA. The channel width in a time slot of each radio is ad-
 124 justed by selecting a different number of subchannels. Thus, the
 125 problem of channel-width adaptation to heterogeneous traffic
 126 demands in various links is converted to another problem, i.e.,
 127 how to allocate subchannels and time slots to different links of
 128 a WMN such that the throughput of the entire network is maxi-
 129 mized. We have made the following contributions in this paper.

- 130 1) Channel-width adaptation is proposed to resolve the issue
 131 of mismatch between link capacity and traffic demands.
 132 Instead of a traditional adaptation mechanism by choos-
 133 ing different available spectrum (i.e., frequency center
 134 and frequency bandwidth), OFDMA-based channel-
 135 width adaptation is proposed as a new mechanism. Based
 136 on this new mechanism, the channel-width adaptation
 137 problem in WMNs is converted into a time slot and
 138 subchannel allocation problem.
- 139 2) An optimization problem is formulated to investigate the
 140 channel-width adaptation problem in WMNs. The corre-
 141 sponding decision problem of this optimization problem
 142 is proved to be NP-complete, which reveals the complex-
 143 ity of channel-width adaptation in WMNs. To reduce the
 144 complexity, a greedy algorithm is proposed to obtain a
 145 suboptimal solution. With the feasible solution from the

greedy algorithm as the initial population, a genetic algo- 146
 rithm (GA) is derived to obtain a near-optimal solution. 147
 Taking the GA as a reference, the greedy algorithm is 148
 shown to achieve comparable performance as that of a 149
 near-optimal solution. 150

- 3) It is shown that the greedy algorithm can be executed 151
 in a distributed way. Thus, this algorithm is incorporated 152
 into a distributed medium access control (MAC) protocol 153
 for channel-width adaptation in OFDMA WMNs. The 154
 MAC protocol is highly adaptive to dynamic network 155
 conditions such as variable traffic demands of wireless 156
 links. Thus, the throughput of the entire network is greatly 157
 improved. 158

The remainder of this paper is organized as follows. The 159
 basic mechanisms and benefits of channel-width adaptation 160
 based on OFDMA are explained in Section II, where related 161
 work is also presented. The time slot and subchannel allo- 162
 cation problem for channel-width adaptation is formulated in 163
 Section III, where a greedy algorithm and a GA are devel- 164
 oped to obtain a near-optimal solution to resource allocation. 165
 Based on the greedy algorithm, a distributed MAC protocol is 166
 designed in Section IV. Performance results are presented in 167
 Section V, and the paper is concluded in Section VI. 168

169 II. CHANNEL-WIDTH ADAPTATION BASED ON 169 170 ORTHOGONAL FREQUENCY-DIVISION MULTIPLE-ACCESS: 170 171 MECHANISMS, BENEFITS, AND RELATED WORK 171

172 A. OFDMA-Based Channel-Width Adaptation Mechanisms 172

We consider a single-radio WMN. Traditionally, the channel 173
 width of a link can be adjusted by selecting: 1) different options 174
 of channel width (e.g., 5, 10, 20, and 40 MHz) available in a ra- 175
 dio; and 2) the center frequency of the operation channel spec- 176
 trum. However, the performance of this approach is impacted 177
 by several drawbacks. First, the granularity of channel-width 178
 adjustment is constrained, and thus, the step size of channel- 179
 width adjustment is limited. For example, the minimum channel 180
 width in an IEEE 802.11 radio must be 5 MHz and the step 181
 size is 5, 10, or 20 MHz. Second, the operation spectrum of a 182
 channel on a radio must be consecutive. 183

In this paper, a different approach is proposed to adjust 184
 channel width. It is based on the capability of subchannels (i.e., 185
 a number of subcarriers) allocation of OFDMA. Compared with 186
 a radio with traditional channel-width adaptation, an OFDMA- 187
 based radio brings several advantages. 188

- 1) It is flexible to adjust channel width to support traffic 189
 demand by selecting a different number of subchannels. 190
- 2) It does not require the spectrum of the selected subchan- 191
 nels to be consecutive, and the step size of channel-width 192
 adaptation can be as fine as one subchannel. 193
- 3) A single OFDMA radio node can support multiple com- 194
 munication links at the same time. 195

196 B. Benefits of the OFDMA-Based Channel-Width Adaptation 196

The benefits of the OFDMA-based channel-width adaptation 197
 are demonstrated in the following example. 198

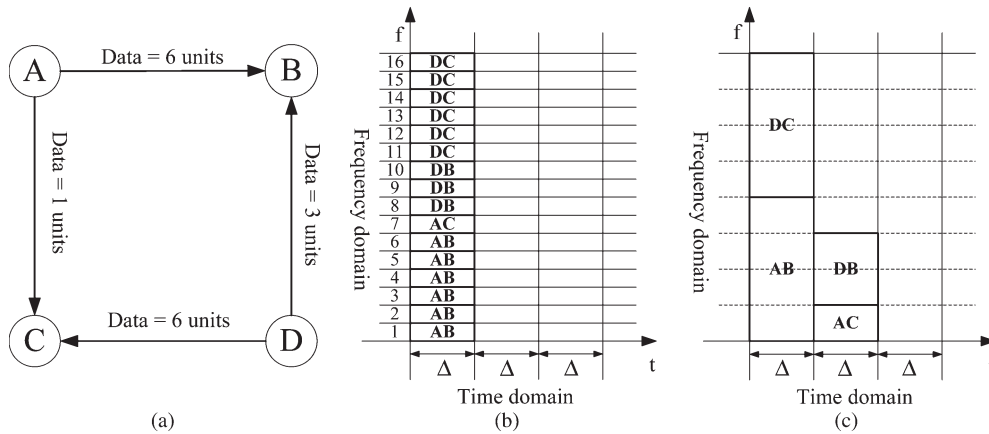


Fig. 1. Benefits of the OFDMA-based channel-width adaptation scheme. (a) Communication topology. (b) OFDMA-based scheme. (c) Traditional scheme.

199 A simple WMN with four nodes A , B , C , and D is consid-
 200 ered in Fig. 1(a), where each node is equipped with one radio.
 201 The links are directional, and the whole spectrum is assumed
 202 to be 40 MHz. In the case of the OFDMA-based channel-width
 203 adaptation mechanism, the whole spectrum is divided into
 204 16 subchannels. For the traditional channel-width adaptation
 205 scheme, channel width can only be selected from $\{5, 10, 20,$
 206 $40\}$ MHz, but the center frequency of a channel can be arbitrar-
 207 ily adjusted. We assume that subchannels are allocated to nodes
 208 slot by slot, and one subchannel per time slot Δ can convey
 209 1 unit traffic demand. In Fig. 1(a), the traffic demands in links
 210 AB , AC , DB , and DC are 6, 1, 3, and 6 units, respectively.

211 Considering the OFDMA-based channel-width adaptation
 212 scheme, the subchannel and time slot allocation is shown in
 213 Fig. 1(b). To support all traffic demands, the time-division
 214 multiple-access (TDMA) frame can be as short as Δ , and the
 215 throughput of the network is $(6 + 1 + 3 + 6)/1 = 16$ (units/ Δ).
 216 Considering the traditional channel-width adaptation scheme,
 217 the channel and time slot allocation is shown in Fig. 1(c). To
 218 support all traffic demands, the TDMA frame needs to be 2Δ .
 219 Thus, the throughput of the network is $(6 + 1 + 3 + 6)/2 =$
 220 8 (units/ Δ).

221 This simple example demonstrates that the network through-
 222 put can be greatly improved by the OFDMA-based channel-
 223 width adaptation scheme for the following reasons: 1) An
 224 OFDMA radio can support several communication links simul-
 225 taneously; and 2) the granularity of channel-width adjustment
 226 of an OFDMA radio can be as small as a subchannel.

227 However, two issues specific to OFDMA-based channel-
 228 width adaptation need to be considered: 1) channel-width
 229 adaptation in both frequency domain and time domain, i.e.,
 230 both time slot and subchannel allocation; and 2) *transmitting*
 231 and *receiving constraint*, i.e., in a time slot, the subchannels
 232 allocated to a radio can only be used for either transmitting or
 233 receiving packets because full duplex wireless communications
 234 [7] are not considered in the OFDMA radio.

235 C. Related Work

236 So far many research papers have addressed the channel
 237 allocation problem in WMNs. For papers on single-radio mul-
 238 tichannel operation [8]–[10], their results are not applicable

to the OFDMA-based channel-width adaptation because fixed
 239 channel width is assumed. For papers on multiradio multichan-
 240 nel operation [11], [12], their algorithms cannot be adopted
 241 either because in the OFDMA-based channel-width adaptation,
 242 there exists a constraint that each node can either transmit
 243 or receive packets on subchannels at one time slot, whereas
 244 this constraint is not considered in the multiradio multichannel
 245 scenarios. In [13], a different channel width is available through
 246 channel combining on a radio for the WMNs. However, the
 247 approach explained in [13] is different from our OFDMA-based
 248 scheme in a single-radio WMN in two aspects: 1) In [13], one
 249 node can only maintain one communication link. However, in
 250 our scheme, one node can simultaneously support several com-
 251 munication links with different nodes; and 2) in [13], a radio
 252 can only use continuous channels, but a radio in our scheme
 253 can transmit on any subchannels in the communication band.
 254 To date, there also exist research results on subcarrier allocation
 255 for OFDMA WMNs. In [14], fair allocation of subcarrier and
 256 power is studied for a specific WMN with one mesh router and
 257 multiple mesh clients. Thus, their point-to-many-points (PMP)
 258 structure is different from our ad hoc network model. In [15],
 259 a joint power-subcarrier-time allocation algorithm is derived
 260 for one cluster of a WMN. In each cluster, the mesh router
 261 is responsible for resource assignment for its mesh clients.
 262 Thus, their network structure is also PMP. More recently, the
 263 resource-allocation problem of multihop OFDMA WMNs has
 264 been conducted in [16]–[19]. However, these papers focus on a
 265 relay-based two-hop network model. Thus, their algorithms are
 266 not applicable to a generic WMN. Consequently, to solve the
 267 subchannel allocation problem for channel-width adaptation in
 268 generic WMNs, new resource-allocation algorithms need to be
 269 derived and an appropriate one must be identified to conduct
 270 channel-width adaptation in a distributed MAC protocol, which
 271 is the focus of this paper. 272

273 III. CHANNEL-WIDTH ADAPTATION ALGORITHMS BASED 274 ON ORTHOGONAL FREQUENCY-DIVISION 275 MULTIPLE-ACCESS 275

Here, the resource-allocation problem considering channel-
 276 width adaptation is formulated first, and then the corresponding
 277 greedy and GAs are derived. 278

279 A. Problem Formulation

280 We consider a WMN consisting of N nodes and L directional
281 links. Each node is equipped with an OFDMA radio. The
282 transmission range of each node is R , and the interference range
283 is R' . The network is modeled as a directional communication
284 graph $G(V, A)$, where V is a set of nodes and A is a set of
285 directed edges. Moreover, $|V| = N$ and $|A| = L$. Thus, for link
286 $l(i, j) \in A$, node $i \in V$ is specified as the sending node and
287 node $j \in V$ is the receiving node.

288 OFDMA is considered in the WMN; hence, a resource unit
289 is a subchannel in a certain time slot. The length of a time slot
290 is fixed, but the TDMA frame length is variable according to
291 the fluctuating traffic demands of all links in the WMN. More
292 specifically, when resource allocation is performed, the total
293 number of time slots is determined such that traffic demands
294 of all links are satisfied within a TDMA frame. This design
295 eliminates the need of admission control, which is a preferred
296 feature of data networks. To be consistent with this design, the
297 traffic demand of a link is not specified as the actual traffic
298 load. Instead, it is specified as the number of resource units per
299 TDMA frame, and each unit represents the data transmitted in
300 one subchannel per time slot, which is the same as the definition
301 in Section II-A. For easy specification of traffic demands, when
302 a node needs to specify the traffic demand of a link, it selects
303 a traffic demand level from the set of $\{1, 2, \dots, M\}$ (units),
304 and the selected level is proportional to its expected actual
305 traffic load. This design of the TDMA frame structure and the
306 resource-allocation mechanism achieves time slotted resource
307 sharing among links of all nodes, which is well suited for data
308 networks.

309 In our OFDMA-based channel-width adaptation mechanism,
310 it is assumed that the whole spectrum is divided into W
311 subchannels and one subchannel supports one unit of traffic
312 demand per time slot. The OFDMA-based radio can transmit
313 data on any combination of these subchannels.

314 We use the protocol model [20] as the interference model.
315 Under this model, a transmission from node i to node j in a time
316 slot is successful if two conditions are satisfied: 1) $d_{ij} \leq R$,
317 where d_{ij} is the distance between node i and node j ; 2) any
318 node k that occupies at least one overlapping subchannel with
319 link $l(i, j)$ and $d_{kj} \leq R'$ is not transmitting. Moreover, a unit
320 of traffic demand means the equivalent data rate that can be
321 supported by a subchannel per time slot. Although the physical
322 layer parameters (such as channel gain and rate adaptation) can
323 impact the data rate of a subchannel per time slot, such impact
324 can be captured by different units of traffic demand. In other
325 words, given the same traffic load, the equivalent units of traffic
326 demand are higher for a lower rate subchannel. Thus, physical
327 layer parameters are not explicitly considered in the protocol
328 model. Due to the OFDMA technique, the problem of channel-
329 width adaptation can be converted into a resource-allocation
330 problem: given traffic demands on different links, how time
331 slots and subchannels are assigned under some constraints such
332 that the total traffic demands are satisfied with the least number
333 of time slots, i.e., the network throughput is maximized. This
334 resource-allocation problem is formulated as follows. First, our
335 objective is to minimize the number of time slots (i.e., the

length of one TDMA frame) that can support the given traffic 336
demands. Suppose that the total number of time slots consumed 337
by the WMN is denoted as T , then the objective function 338
becomes 339

$$\text{Minimize } T. \quad (1)$$

Obviously, T lies in the positive integer set, i.e., 340

$$T \in \{1, 2, \dots\}. \quad (2)$$

To help determine time slot and subchannel allocation for 341
each directional link, $X(i, j, t, s)$ is used to denote the alloca- 342
tion status of link $l(i, j)$ in time slot t and subchannel s . Since 343
 $X(i, j, t, s) \in \{0, 1\}$, we have the following constraint: 344

$$\begin{aligned} X(i, j, t, s) &\in \{0, 1\} \\ \forall l(i, j) \in A \quad \forall t = 1, 2, \dots, T \quad \forall s = 1, 2, \dots, W. \end{aligned} \quad (3)$$

To capture potential interference between links, we need a 345
link interference constraint described as follows: 346

$$\begin{aligned} X(i, j, t, s) + X(p, q, t, s) &\leq 1 \\ \forall l(i, j) \in A \quad \forall t = 1, 2, \dots, T \quad \forall s = 1, 2, \dots, W \\ \forall l(p, q) \in I_{l(i, j)} \end{aligned} \quad (4)$$

where $I_{l(i, j)}$ is the interference set of link $l(i, j)$. 347

Since each mesh node has a single radio, it either transmits 348
or receives on all the occupied subchannels in the same time 349
slot. Thus, for a certain link $l(i, j)$, we have the following 350
transmitting and receiving constraint (i.e., *Tx/Rx constraint*): 351

$$\begin{aligned} X(i, j, t, s) \times \left[X(i, j, t, s) + \sum_{f=1}^W \sum_{p \in \text{in}(i)} X(p, i, t, f) \right. \\ \left. + \sum_{g=1}^W \sum_{q \in \text{out}(j)} X(j, q, t, g) \right] &\leq 1 \\ \forall l(i, j) \in A \quad \forall t = 1, 2, \dots, T \quad \forall s = 1, 2, \dots, W \end{aligned} \quad (5)$$

where $\text{in}(i)$ is a set of nodes that send data to node i . Similarly, 352
 $\text{out}(j)$ is the set of nodes that receive data from node j . 353

Finally, to satisfy the traffic demand of each link $l(i, j) \in A$, 354
we need to consider the *traffic demand constraint* 355

$$\begin{aligned} \sum_{t=1}^T \sum_{s=1}^W X(i, j, t, s) &\geq D(i, j) \\ D(i, j) &\in \{1, 2, \dots, M\} \end{aligned} \quad (6)$$

where $D(i, j)$ represents the units of traffic demand on link 356
 $l(i, j)$. This constraint means that each link must be assigned 357
with enough time slots and subchannels to support its traffic 358
demand. 359

Consequently, we have formulated the optimization problem 360
of time slot and subchannel allocation for OFDMA-based 361
channel-width adaptation. We call this problem the single- 362
radio OFDMA-based resource-allocation (SRORA) problem. 363
In summary, SRORA needs to optimize the objective in (1), 364
subject to constraints in (2)–(6). In the following theorem, we 365
prove that SRORA is NP-complete. 366

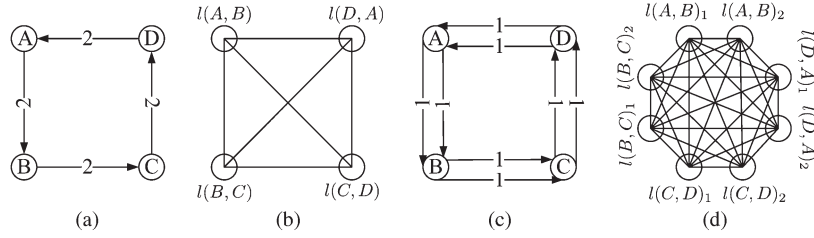


Fig. 2. (a) Communication graph $G(V, A)$, which consists of four directional communication links. Each link has 2 units of traffic demands. Based on the protocol interference model, $G(V, A)$ is converted into the interference graph G' in (b), where each vertex represents a directional communication link in $G(V, A)$. (c) Split communication graph of $G(V, A)$. It is constructed by splitting a communication link in $G(V, A)$ into several links, each with one unit of traffic demand, e.g., $l(A, B)$ in $G(V, A)$ has two units of traffic demands; hence, it is split into $l(A, B)_1$ and $l(A, B)_2$ in G_{split} , each with one unit of traffic demand. (d) Interference graph of the split communication graph G_{split} . (a) $G(V, A)$. (b) G' . (c) G_{split} . (d) G'_{split} .

367 *Theorem 1:* In SRORA, the decision problem of verifying
368 whether K time slots are enough to satisfy the total traffic
369 demands is NP-complete.

370 *Proof:* First, for any candidate solution of time slot and
371 subchannel allocation, whether all the constraints are satisfied
372 can be verified in polynomial time. Thus, the decision problem
373 in SRORA is NP. Second, we consider the special case of
374 SRORA by setting $W = 1$ and $D(i, j) = 1$ for all links. Using
375 the protocol interference model, we convert the directional link
376 $l(i, j) \in A$ in the communication graph $G(V, A)$ into the vertex
377 in the corresponding interference graph G' , as shown in Fig. 2.
378 Based on the interference graph G' , each link $l(i, j)$ in the
379 communication graph $G(V, A)$ can construct an interference set
380 $I_{l(i, j)}$. Since in this special case only one subchannel and one
381 unit of traffic demand are considered for each link, only one
382 time slot is needed in a frame to satisfy *traffic demand con-*
383 *straint* (6). To satisfy *link interference constraint* (4), any link
384 in $I_{l(i, j)}$ must be assigned a different time slot from that of link
385 $l(i, j)$. In this special case, when *link interference constraint* (4)
386 is satisfied, *Tx/Rx constraint* (5) is also automatically satisfied
387 due to the two facts: 1) The links $l(p, i)$ where $p \in \text{in}(i)$ and
388 links $l(j, q)$ where $q \in \text{out}(j)$ are in set $I_{l(i, j)}$; and 2) the
389 link in $I_{l(i, j)}$ is assigned with a different time slot from the
390 link $l(i, j)$. Therefore, the problem of determining whether K
391 time slots are enough to support the traffic demands of all
392 links in the communication graph $G(V, A)$ is equivalent to the
393 problem of checking whether K colors are sufficient to color
394 the vertices in the corresponding interference graph G' . We
395 know that the latter problem is NP-complete [21], which means
396 that every problem in NP is reducible to the decision problem of
397 SRORA in polynomial time. As a result, the decision problem
398 of SRORA (in the special case) is NP-complete. In the general
399 case (with W subchannels and $D(i, j)$ traffic demand), the
400 decision problem is also NP-complete. \square

401 B. Greedy Algorithm

402 Since the problem SRORA is NP-complete, a low-
403 complexity greedy algorithm is proposed for the SRORA prob-
404 lem, and we call it GR-SRORA. In our greedy algorithm, links
405 are assigned with time slot and subchannel in a certain sequen-
406 tial order just like coloring the vertices in the corresponding
407 interference graph. However, here we also need to consider
408 *Tx/Rx constraint*.

GR-SRORA is described in Algorithm 1. It works as 409
follows. 410

- 411 1) Lines 2–15 specify the procedures of assigning the 411
time slot and subchannel to link $l(i, j)$ considering both 412
link interference constraint and *Tx/Rx constraint*. The 413
resource-allocation status table of link $l(i, j)$, denoted by 414
 $\Phi(i, j, t, s)$, captures *link interference constraint*. More 415
specifically, for any t and s , if $\Phi(i, j, t, s) = 1$, it means 416
that subchannel s in time slot t is occupied by a link in 417
the interference set of link $l(i, j)$ (i.e., $I_{l(i, j)}$). The single- 418
radio OFDMA constraint table of link $l(i, j)$, denoted by 419
 $\Psi(i, j, t)$, captures *Tx/Rx constraint*. More specifically, 420
for any t , if $\Psi(i, j, t) = 1$, it means that link $l(i, j)$ cannot 421
transmit on any subchannel in time slot t . 422
- 423 2) Lines 16–19 are executed after a link assignment. Two ta- 423
bles ($\Phi(p, q, t, s)$ and $\Psi(p, q, t)$) of each link are updated 424
and will be used in the next link assignment. 425
- 426 3) Line 21 is used to determine T_{greedy} , which is the total 426
number of time slots consumed by the network following 427
the greedy algorithm. 428

The performance of the greedy algorithm GR-SRORA is 429
analyzed as follows. We denote the minimum number of time 430
slots consumed in SRORA and the greedy algorithm GR- 431
SRORA as T_{optimal} and T_{greedy} , respectively. Based on the 432
split graph G_{split} of the original communication graph $G(V, A)$ 433
and the split interference graph G'_{split} in Fig. 2, the relationship 434
between T_{optimal} and T_{greedy} is shown in Theorem 2. 435

Algorithm 1 GR-SRORA

Input:

- Communication graph $G(V, A)$ 438
- Resource consumption status table of link $l(i, j)$: 439
 $\Phi(i, j, t, s)$ 440
- Single-radio OFDMA constraint table of link $l(i, j)$: 441
 $\Psi(i, j, t)$ 442
- Traffic demand on link $l(i, j)$: $D(i, j)$ 443
- Number of total subchannels: W 444

Output:

- Network time slot consumption: T_{greedy} 445
- The maximum time slot assigned to link $l(i, j)$: $T_{l(i, j)}$ 447
- Time slot and subchannel allocation result for link $l(i, j)$: 448
 $X(i, j, t, s)$ 449

450 **Initialization:**
 451 • $\Phi(i, j, t, s) = 0$
 452 • $\Psi(i, j, t) = 0$
 453 • $T_{\text{greedy}} = 0$
 454 • $T_{l(i,j)} = 0$
 455 1: **for all** $l(i, j) \in A$ **do**
 456 2: **for** $t = 1$ to $+\infty$ **do**
 457 3: **if** $D(i, j) == 0$ **then**
 458 4: **Break;**
 459 5: **end if**
 460 6: **if** $\Psi(i, j, t) \neq 1$ **then**
 461 7: **for** $s = 1$ to W **do**
 462 8: **if** $D(i, j) > 0$ && $\Phi(i, j, t, s) == 0$ **then**
 463 9: $X(i, j, t, s) = 1$
 464 10: $D(i, j) = D(i, j) - 1$
 465 11: $T_{l(i,j)} = t$
 466 12: **end if**
 467 13: **end for**
 468 14: **end if**
 469 15: **end for**
 470 16: **for all** $l(p, q) \in A$ **do**
 471 17: Update $\Phi(p, q, t, s)$
 472 18: Update $\Psi(p, q, t)$
 473 19: **end for**
 474 20: **end for**
 475 21: $T_{\text{greedy}} = \max_{l(i,j) \in A} T_{l(i,j)}$
 476 22: **Stop.**

477 *Theorem 2:* For the optimal solution of the problem SRORA
 478 T_{optimal} and the greedy solution of GR-SRORA T_{greedy} ,
 479 $\lceil (\chi(G'_{\text{split}})/W) \rceil \leq T_{\text{optimal}} \leq T_{\text{greedy}} \leq T_{\text{max}} = \delta(G'_{\text{split}}) + 1$,
 480 where $\lceil \cdot \rceil$ is the ceiling function, $\delta(\cdot)$ is the maximum degree
 481 of a graph, and $\chi(\cdot)$ is the chromatic number of a graph. More-
 482 over, G'_{split} is the interference graph constructed by splitting a
 483 communication link in $G(V, A)$ into separate links, each with
 484 one unit traffic demand.

485 *Proof:* The proof consists of two parts. First, we derive
 486 the lower bound of T_{optimal} by looking into the property of
 487 T_{optimal} . In the communication graph $G(V, A)$, each directional
 488 link $l(i, j)$ (with traffic demand $D(i, j)$) is split into $D(i, j)$ vir-
 489 tual directional links between node i and node j to construct the
 490 split communication graph G_{split} , as shown in Fig. 2(c). Based
 491 on the protocol interference model, the split communication
 492 graph G_{split} is converted into its corresponding interference
 493 graph G'_{split} , as shown in Fig. 2(d). If each vertex of G'_{split} is
 494 greedily colored, i.e., assigning different time slot–subchannel
 495 pairs to interfering virtual links G_{split} , then each link in
 496 communication graph $G(V, A)$ certainly satisfies the *link inter-*
 497 *ference constraint*. The minimum number of colors (i.e., time
 498 slot–subchannel pairs) that G'_{split} consumes is the chromatic
 499 number $\chi(G'_{\text{split}})$ [22]. Since W subchannels are available for
 500 each time slot, the minimum number of consumed time slots
 501 becomes $\lceil (\chi(G'_{\text{split}})/W) \rceil$, when only *link interference con-*
 502 *straint* is taken into account. However, in SRORA, there exists
 503 the *Tx/Rx constraint*; hence, the optimal number of time slots
 504 (i.e., T_{optimal}) must be larger than or equal to $\lceil (\chi(G'_{\text{split}})/W) \rceil$.
 505 In other words, $\lceil (\chi(G'_{\text{split}})/W) \rceil \leq T_{\text{optimal}}$ holds.

Second, we derive the upper bound of T_{optimal} by exploring
 the property of T_{greedy} . We consider the worst case where
 there exists only one subchannel (i.e., $W = 1$). Given any
 link assignment order $\vec{\mathcal{L}}$ taken by GR-SRORA, there exists a
 corresponding greedy coloring order in G'_{split} . For any greedy
 coloring order in G'_{split} , the number of colors that are needed is
 at most $\delta(G'_{\text{split}}) + 1$ [23]. Since the number of colors in G'_{split}
 is exactly equal to the number of time slots needed in the worst
 case communication graph, i.e., $T_{\text{greedy}}^{\text{worst}}(\vec{\mathcal{L}})$, thus, for any link
 assignment order $\vec{\mathcal{L}}$, the number of time slots that are consumed
 is upper bounded by $T_{\text{max}} = \delta(G'_{\text{split}}) + 1$. In general, the
 number of subchannels W is usually a constant greater than 1.
 Thus, for any link assignment order $\vec{\mathcal{L}}$, the total number of time
 slots needed by GR-SRORA $T_{\text{greedy}}(\vec{\mathcal{L}})$ is equal or smaller than
 $T_{\text{greedy}}^{\text{worst}}(\vec{\mathcal{L}})$. Thus, $T_{\text{greedy}} \leq T_{\text{max}} = \delta(G'_{\text{split}}) + 1$. 520

Combining the lower bound and the upper bound, we have
 $\lceil (\chi(G'_{\text{split}})/W) \rceil \leq T_{\text{optimal}} \leq T_{\text{greedy}} \leq T_{\text{max}} = \delta(G'_{\text{split}}) + 1$,
 which proves Theorem 2. \square 523

The complexity of the GR-SRORA is analyzed as follows.
 In GR-SRORA, the number of links L is a variable, but sub-
 channel number W and traffic demand upper bound M for each
 link are constants. In Algorithm 1, lines 2–15 are for assigning
 time slots and subchannels to link $l(i, j)$. Its complexity is
 $\mathcal{O}(T_{\text{max}})$, where T_{max} is the upper bound of T_{greedy} . As shown
 in Theorem 2, $T_{\text{max}} = \delta(G'_{\text{split}}) + 1$. Since $\delta(G'_{\text{split}}) + 1 \leq$
 $M \times L + 1$, hence, $T_{\text{max}} \leq M \times L + 1$. Thus, the complexity
 from lines 2–15 is $\mathcal{O}(L)$. Lines 16–19 are to update $\Phi(i, j, t, s)$
 and $\Psi(i, j, t)$. The complexity is $\mathcal{O}(L)$. Thus, considering lines
 1–22, the complexity is $L \times (\mathcal{O}(L) + \mathcal{O}(L))$. Therefore, the
 total complexity is $\mathcal{O}(L^2)$. 535

C. GA

Since the greedy algorithm, i.e., GR-SRORA, usually can
 only obtain the suboptimal solution, we adopt a GA to obtain
 a near-optimal result as a theoretical reference for our greedy
 algorithm. 540

To apply the GA, the number of decision variables
 $X(i, j, t, s)$ in the optimization problem SRORA needs to be
 constant. Since for a certain network the number of links L
 and the number of subchannels W are constants, we also need
 to fix the total time slots for assignment so that the number
 of $X(i, j, t, s)$ will be fixed. From the proof of Theorem 2,
 T_{optimal} is upper bounded by $T_{\text{max}} = \delta(G'_{\text{split}}) + 1$ for a given
 communication graph $G(V, A)$. With this bound, the problem
 SRORA is reformulated as follows: 549

Minimize T .

$$\text{s.t.} \begin{cases} X(i, j, t, s) + X(p, q, t, s) \leq 1 \\ \left[X(i, j, t, s) + \sum_{f=1}^W \sum_{p \in \text{in}(i)} X(p, i, t, f) \right. \\ \left. + \sum_{g=1}^W \sum_{q \in \text{out}(j)} X(j, q, t, g) \right] \times X(i, j, t, s) \leq 1 \\ \sum_{t=1}^{T_{\text{max}}} \sum_{s=1}^W X(i, j, t, s) \geq D(i, j) \\ X(i, j, t, s) \in \{0, 1\} \\ \forall l(i, j) \in A \quad \forall s = 1, 2, \dots, W \\ \forall l(p, q) \in I_{l(i,j)} \quad \forall t = 1, 2, \dots, T_{\text{max}}. \end{cases}$$

550 The objective T is the maximum occupied time slot in the
 551 network and is calculated with decision variable $X(i, j, t, s)$ as
 552 $T = \max_{t \in \{1, 2, \dots, T_{\max}\}} t$, subject to $\max_{l(i, j) \in A, s \in \{1, 2, \dots, W\}}$
 553 $X(i, j, t, s) \neq 0$. The previous optimization problem is exactly
 554 the same as SRORA, except that the range of t is upper bounded
 555 by T_{\max} instead of T . Thus, its complexity is the same as
 556 SRORA, i.e., it is also NP-complete.

557 Based on this new formulation, a GA is developed for
 558 SRORA. We call it GA-SRORA. Different from classic opti-
 559 mization methods such as gradient-based approaches, GA is
 560 well suited for integer programming problems. Although there
 561 is no absolute guarantee for the GA-SRORA to obtain an
 562 optimal solution, the algorithm can be executed for sufficient
 563 time to reach a near-optimal solution.

564 GA evolves its generation into the next generation via three
 565 essential steps: reproduction, crossover, and mutation. Thus,
 566 GA-SRORA is executed according to the following steps.

- 567 1) Initialize Population: The population of our algorithm
 568 GA-SRORA consists of chromosomes. Each chromo-
 569 some is represented by $X(i, j, t, s)$ of all links.
- 570 2) Evaluation and Fitness Assignment: For every chromo-
 571 some, its fitness needs to be minimized in GA-SRORA.
 572 The fitness captures the objective function and the con-
 573 straints in the reformulated SRORA problem. As a result,
 574 the fitness is described as

Fitness

$$\begin{aligned}
 &= T + P \times (C_1 + C_2 + C_3) \\
 C_1 &= \sum_{l(i, j) \in A} \max \left[0, 1 - \sum_{t=1}^{T_{\max}} \sum_{s=1}^W X(i, j, t, s) / D(i, j) \right] \\
 C_2 &= \sum_{l(i, j) \in A} \sum_{l(p, q) \in I_{l(i, j)}} \sum_{t=1}^{T_{\max}} \sum_{s=1}^W \max \\
 &\quad \times [0, X(i, j, t, s) + X(p, q, t, s) - 1] \\
 C_3 &= \sum_{l(i, j) \in A} \sum_{t=1}^{T_{\max}} \sum_{s=1}^W \max \\
 &\quad \times \left[0, \left(X(i, j, t, s) + \sum_{f=1}^W \sum_{p \in \text{in}(i)} X(p, i, t, f) \right. \right. \\
 &\quad \left. \left. + \sum_{g=1}^W \sum_{q \in \text{out}(j)} X(j, q, t, g) \right) X(i, j, t, s) - 1 \right]
 \end{aligned}$$

575 where T is the maximum occupied time slot in the
 576 network and is obtained with $X(i, j, t, s)$, P as a penalty
 577 parameter. C_1 , C_2 , and C_3 are derived from *traffic de-*
 578 *demand constraint*, *link interference constraint*, and *Tx/Rx*
 579 *constraint*, respectively.

- 580 3) Reproduction: According to the fitness, better chromo-
 581 somes are copied and worse chromosomes are removed,
 582 whereas holding population size constant. A fair selection
 583 is applied to generate “winners” and put them into the
 584 “mating pool.”
- 585 4) Crossover: Parent chromosomes swap a subset of their
 586 strings, generating two new chromosomes called children.

- 587 5) Mutation: A new chromosome is generated by changing
 588 value of one bit in its string. This step reduces the chance
 589 of falling into the local optimal point.
- 590 6) Steps 2–5 are repeated for U rounds to obtain a relatively
 591 stable solution.

The complexity of the GA-SRORA can be derived similarly
 592 to Algorithm 1. For iteration rounds U , population size V , and
 593 link number L , the complexity of GA-SRORA is $\mathcal{O}(UVL^3)$. 594

IV. DISTRIBUTED MEDIUM ACCESS CONTROL FOR ORTHOGONAL FREQUENCY-DIVISION MULTIPLE-ACCESS-BASED CHANNEL-WIDTH ADAPTATION

595 Here, a distributed MAC protocol is designed based on the
 596 greedy algorithm for OFDMA-based channel-width adaptation. 600

A. Distributed Operation of the Greedy Algorithm

601 Four information tables are maintained by every node i :
 602 1) $Q_{\text{in}}(i, p, q)$, which indicates whether subchannel q in time
 603 slot p is occupied by a receiving link (i.e., incoming link) of a
 604 node in the interference range of node i ; 2) $Q_{\text{out}}(i, p, q)$, which
 605 indicates whether subchannel q in time slot p is occupied by a
 606 sending link (i.e., outgoing link) of a node in the interference
 607 range of node i ; 3) $O_{\text{in}}(i, t)$, which indicates whether time slot
 608 t is occupied by any receiving link of node i ; and 4) $O_{\text{out}}(i, t)$,
 609 which indicates whether time slot t is occupied by any sending
 610 link of node i . How such information is collected is explained
 611 in Section IV-C and D. 612

For a given link $l(i, j)$, sending node i is responsible for
 613 assigning time slots and subchannels to support a given number
 614 of units (denoted as $D(i, j)$) in a TDMA frame. With these
 615 variables, resource allocation of link $l(i, j)$ is executed as
 616 follows. 617

- 618 1) Information fusion: Based on the protocol interference
 619 model, any receiving link of a node located in the interfer-
 620 ence range of node i or any sending link of a node located
 621 in the interference range of node j potentially interferes
 622 with link $l(i, j)$; hence, node i needs to communicate with
 623 node j to collect all the resource-allocation information
 624 by combining tables $Q_{\text{in}}(i, p, q)$ and $Q_{\text{out}}(j, p, q)$ before
 625 resource allocation is conducted. Due to the single-radio
 626 OFDMA *Tx/Rx constraint*, node i also needs to obtain
 627 table $O_{\text{out}}(j, t)$ from node j , and then determines which
 628 time slot is still available by checking $O_{\text{in}}(i, t)$ and
 629 $O_{\text{out}}(j, t)$. 629
- 630 2) Time slot and subchannel allocation: For the first time
 631 slot, node i assigns the unoccupied subchannels to link
 632 $l(i, j)$ to support the traffic demands. If the first time slot
 633 is not enough, it goes to the second time slot. This process
 634 is repeated until the sum of the assigned subchannels
 635 can support the traffic demand of link $l(i, j)$. During
 636 this period, any link $l(p, q) \in I_{l(i, j)}$ (i.e., $l(p, q)$ is any
 637 receiving link of a node located in the interference range
 638 of node i or any sending link of a node located in the
 639 interference range of node j) cannot conduct resource
 640 allocation simultaneously. 640

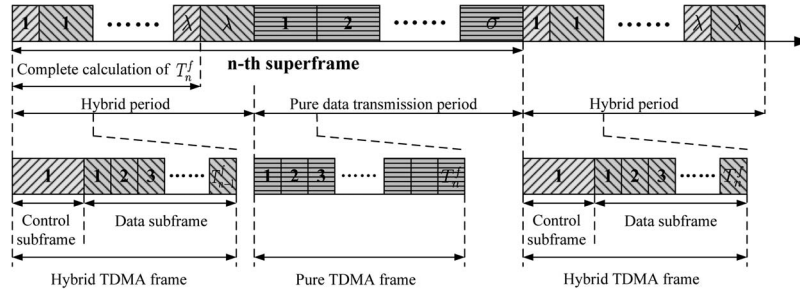


Fig. 3. Frame structure.

3) Information table update: After resource allocation of link $l(i, j)$, all nodes in the interference range of node i and node j update their information tables immediately.

To support the aforementioned mechanisms, the control messages need to be received within the interference range. To this end, the lowest transmission rate is adopted by control messages.

Since every node contends to assign resources to its outgoing links in a greedy way, two nodes that are far away enough can conduct resource allocation simultaneously. As a result, resource allocation in the entire WMN is conducted in a distributed way and is thus called distributed GR-SRORA (DGR-SRORA). Based on this distributed resource-allocation process, a distributed multisubchannel TDMA MAC protocol is developed in the following sections.

B. Frame Structure

The new MAC protocol works in a hybrid way, as shown in Fig. 3. In each superframe, a new resource allocation is carried out in λ control subframes, and data transmissions proceed on the assigned time slots and subchannels.

A superframe includes two parts, namely, hybrid period and pure data transmission period. The hybrid period consists of λ hybrid TDMA frames, where λ is a constant and must be set large enough for all the nodes to complete resource allocation. A hybrid TDMA frame is composed of two subframes: control subframe and data subframe. Each consists of a number of time slots. The control subframe is used for resource allocation. The data subframe is used for data transmission. The pure data transmission period consists of σ pure TDMA frames, where σ is a constant. These TDMA frames are only used for data transmission.

As shown in Fig. 3, in the n th superframe, the length of the data subframe in the hybrid period is T_{n-1}^f , which is determined in the $(n-1)$ -th superframe. In the hybrid period of the n th superframe, our resource-allocation algorithm determines a new length of a TDMA frame T_n^f . This new value updates the length of a pure TDMA frame in the pure data transmission period of the n th superframe. It also determines the length of the data subframe in the hybrid period of the $(n+1)$ -th superframe. As a result, in Fig. 3, the frame lengths in the left hybrid TDMA frame and the right hybrid TDMA frame are equal to T_{n-1}^f and T_n^f , respectively.

In the control subframe of the hybrid period, each node uses an request-to-send/clear-to-send mechanism to contend for time slots' and subchannels' allocation. In all TDMA frames

for data transmission, each node adopts carrier-sense multiple access/collision avoidance to access the assigned time slots and subchannels. This can prevent collisions due to allocation error or out-of-network interference. As a result, our MAC protocol is actually a TDMA MAC overlaying CSMA/CA.

C. Distributed Resource-Allocation Procedure

The control subframe in Fig. 3 is used to signal distributed resource allocation. Control messages are sent with the lowest transmission rate using all subchannels. For resource assignment of link $l(i, j)$, the negotiation between node i and node j follows this procedure.

- 1) Node i sends a request-to-assign (RTA) packet to node j . All nodes except node j in the sensing range of node i keep quiet.
- 2) Upon receiving the RTA packet, node j sends node i a clear-to-assign (CTA) packet, which contains $Q_{out}(j, p, q)$ and $O_{out}(j, t)$. All nodes except node i in the sensing range of node j keep quiet.
- 3) Upon receiving the CTA packet, node i relies on tables $Q_{in}(i, p, q)$, $Q_{out}(j, p, q)$, $O_{in}(i, t)$, and $O_{out}(j, t)$ to assign time slots and subchannels to link $l(i, j)$. Then, node i broadcasts an announcement (ANN) packet, which contains the assignment result for link $l(i, j)$, to all nodes in its interference range.
- 4) Upon receiving the ANN packet, all nodes in the interference range of node i update their tables. Node j also broadcasts an ANN packet to all nodes in its interference range, and then such receiving nodes update their information tables.

An example of resource-allocation procedure is explained next. The signaling messages are transmitted in the lowest rate to cover all the nodes in the interference range, and the exchange procedure is shown in Fig. 4.

- 1) Node A starts to assign time slots and subchannels for link $l(A, B)$. It broadcasts an RTA packet to node B . Node C and node D can receive the signaling packet; hence, they keep quiet.
- 2) Node B receives the RTA packet and then broadcasts a CTA packet, which contains $Q_{out}(B, p, q)$ and $O_{out}(B, t)$, to node A . Nodes A and C can receive this packet, but node D can only sense it.
- 3) Node A receives the CTA packet and broadcasts an ANN packet, which contains the assignment result for link $l(A, B)$. Node B receives this packet, but nodes C and D can only sense it.

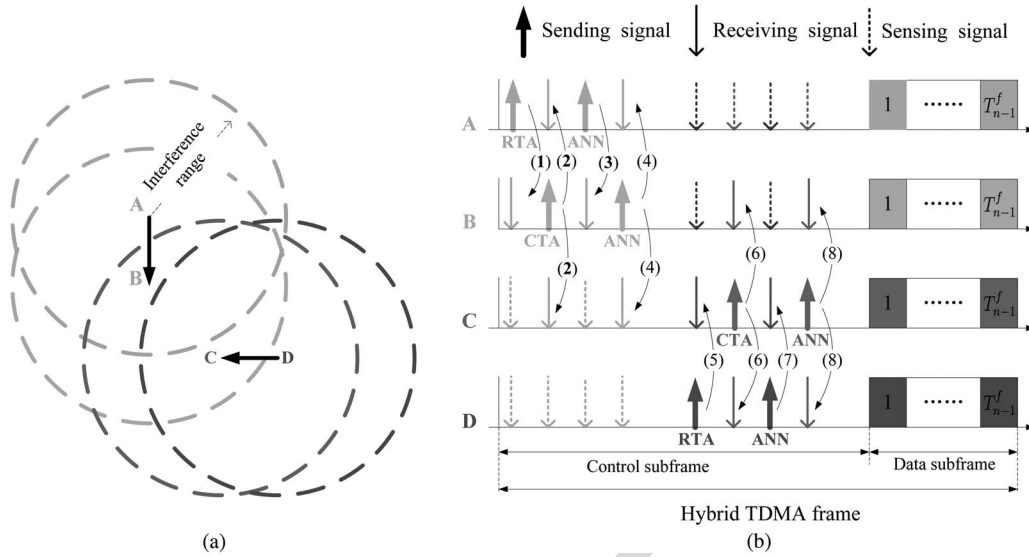


Fig. 4. Operation of the MAC protocol: An example. (a) Topology. (b) Resource negotiation.

- 731 4) When node *B* receives the ANN packet, it updates its
 732 own information tables and rebroadcasts the ANN packet.
 733 Nodes *A* and *C* receive it and update their tables, but node
 734 *D* can only sense it.
 735 5) Node *D* starts to assign time slots and subchannels for
 736 link $l(D, C)$. It broadcasts an RTA packet to node *C*.
 737 Node *A* and node *B* can sense the signaling; hence, they
 738 keep quiet.
 739 6) Node *C* receives the RTA packet and then broad-
 740 casts a CTA packet, which contains $Q_{out}(C, p, q)$ and
 741 $O_{out}(C, t)$, to node *D*. Node *D* and node *B* can receive
 742 this packet, but node *A* can only sense it.
 743 7) Node *D* receives the CTA packet and broadcasts an
 744 ANN packet, which contains the allocation result of link
 745 $l(D, C)$. Node *C* receives this packet, but node *A* and
 746 node *B* can only sense it.
 747 8) When node *C* receives the ANN packet, it updates its
 748 own information tables and rebroadcasts the ANN packet.
 749 Nodes *D* and *B* receive it and update their information
 750 tables, but node *A* can only sense it.

751 In the distributed algorithm, every node determines its own
 752 time slot. Thus, the largest time slot in one node may be dif-
 753 ferent from that of another node. To avoid inconsistent TDMA
 754 frame in different links, the largest time slot in the allocation
 755 must be known to all nodes. This can be done by the following
 756 simple procedure. When a node gets resource-allocation infor-
 757 mation from another node, it compares its largest time slot with
 758 that in the allocation information. If its own value is smaller,
 759 it needs to update its largest time slot number and broadcast
 760 the updated information to its neighbors; otherwise, no action
 761 is needed.

762 D. Enhancement for Multiple Interference Domains

763 The aforementioned protocol is effective for the single in-
 764 terference domain because every time only one link is in the
 765 resource-allocation process and other nodes can hear signaling
 766 messages and keep quiet. However, in the case of multiple

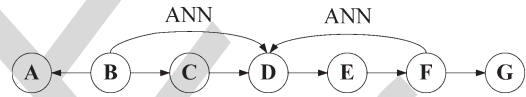


Fig. 5. ANN packet collision may occur in the case of multiple interference domains.

interference domains, there exist collisions in ANN packets. 767
 For example, in Fig. 5, node *B* and node *F* successfully make 768
 reservation for link $l(B, A)$ and link $l(F, G)$ by exchanging 769
 RTA and CTA packets. However, it is possible that the ANN 770
 packets broadcast by node *B* and node *F* simultaneously and 771
 interfere each other at node *D*. Thus, node *D* cannot receive 772
 the ANN packet, which leads to errors in the following resource 773
 assignment in other links. To reduce the probability of colli- 774
 sions in ANN packets, we propose a scheme as follows. During 775
 the resource-allocation process of link $l(i, j)$, node *i* and node 776
j exchange RTA and CTA packets as usual. The process of 777
 broadcasting ANN packets is modified to reduce the collision 778
 probability: 1) Node *i* and node *j* broadcast ANN packets in 779
 turn for K_{ANN} rounds instead of only one round; and 2) be- 780
 fore broadcasting an ANN packet, the sending node randomly 781
 chooses a waiting time in the backoff window W_{ANN} and de- 782
 lays the ANN packet transmission for the chosen waiting time. 783

Although this scheme cannot guarantee collision-free ANN 784
 packets, the collision probability dramatically drops with the 785
 increased K_{ANN} and W_{ANN} . It should be noted that how 786
 to design an effective distributed MAC protocol in multiple 787
 interference domains still remains a challenging problem. 788

789 V. PERFORMANCE RESULTS

Here, MATLAB simulations are carried out to evaluate our 790
 algorithms and protocols developed in previous sections. Since 791
 the objective of our algorithms and protocols is to leverage 792
 channel-width adaptation to efficiently support diverse traffic 793
 demands in different links of a WMN, transmission rate in 794
 different links is assumed to be homogeneous. Performance 795
 results from such a setting provide a better demonstration about 796

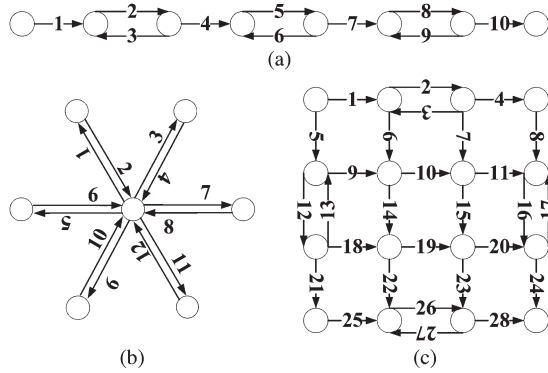


Fig. 6. Simple topologies.

797 how channel-width adaptation improves throughput; the impact
798 from heterogeneous link rates is eliminated. In simulations, the
799 homogeneous link rate is equal to 54 Mb/s when the band-
800 width is 20 MHz. The total available bandwidth is 40 MHz;
801 hence, the corresponding link rate using a whole spectrum
802 is 108 Mb/s. Moreover, a single radio is considered in each
803 mesh node.

804 In our OFDMA-based channel-width adaptation scheme, the
805 whole spectrum is divided into 64 subchannels and the length
806 of a time slot is 5 ms. We assume that one subchannel per time
807 slot can transmit 1 unit of traffic demand. If a link is assigned
808 two subchannels every three time slots, then its throughput
809 is $(2/3) \times (108/64) = 1.125$ Mb/s. The network throughput is
810 defined as the ratio of the total supported traffic demands over
811 the length of a TDMA frame.

812 To fully evaluate our algorithm and protocols, different net-
813 work topologies are considered in the following sections. The
814 details of network setup and the corresponding traffic demands
815 are specified separately for each topology.

816 A. Simple Topologies

817 The greedy algorithm and GA are evaluated under three
818 simple topologies in Fig. 6. In each topology, the link ID is
819 marked in the figure, and all the links have the same length,
820 which represents the communication range. The interference
821 range is set twice the communication range.

822 For each link, the traffic demand is uniformly distributed in
823 $\{1, \dots, 128\}$ (units).

824 For each topology, we evaluate the network throughput
825 that can be achieved in a WMN with available bandwidth
826 of 40 MHz. The performance results of our channel-width
827 adaptation algorithms (i.e., GR-SRORA and GA-SRORA) are
828 compared with that achieved by the single-radio traditional
829 channel-width adaptation (SRTCWA) scheme and also with
830 that achieved by the single-radio fixed channel-width (SRFCW)
831 scheme. SRTCWA and SRFCW are executed following the
832 same procedure as GR-SRORA (i.e., greedily assign time slot
833 and channel to all the links in the same order as GR-SRORA)
834 but consider different constraints. In SRTCWA, there are four
835 options of channel width (i.e., 5, 10, 20, and 40 MHz), and the
836 center frequency of each channel can be adjusted. In SRFCW,
837 the radio on each node uses a 20-MHz channel. To be fair in
838 comparison, two orthogonal channels (i.e., totally 40 MHz) are

available in SRFCW for parallel links in the same interference
839 domain. 840

In the string topology, as shown in Fig. 7(a), on average, the
841 network throughput of GR-SRORA is 19.2% higher than that
842 achieved by SRTCWA and 30.8% higher than that of SRFCW.
843 In this network structure, the throughput improvement is not
844 significant due to lack of PMP structure in the string topology. 845

In the star topology, as shown in Fig. 7(b), on average, 846
the network throughput of GR-SRORA is 54.5% higher than
847 that of SRTCWA and 136.4% higher than that of SRFCW. 848
The improvement is significant because our OFDMA-based
849 channel-width adaptation scheme is very suitable for explor-
850 ing channel-width adaptive concurrent transmissions in a star
851 network structure. 852

In the grid topology, as shown in Fig. 7(c), on average, the
853 network throughput of GR-SRORA is 19.3% higher than that
854 of SRTCWA and 29.8% higher than that of SRFCW. 855

As shown in Fig. 7, the greedy algorithm achieves nearly
856 the same throughput as that of the GA-based algorithm, which
857 indicates that the greedy algorithm is effective to obtain a
858 near-optimal solution to the channel-width adaptation problem
859 in WMNs. 860

B. Randomized Topology 861

Our distributed MAC protocol is also evaluated in a ran- 862
domized topology. The communication range of each node is
863 100 m, the interference range is 200 m, and the sensing range is
864 300 m. The RTA and CTA packets have a length of 120 bytes,
865 and the ANN packet has a length of 30 bytes. As explained in
866 Section IV, the lowest transmission rate is adopted to send these
867 packets, and it is set to 6 Mb/s. 868

1) *Single Interference Domain Scenario*: In this scenario, 869
nodes are randomly distributed within a circle with a diameter
870 of 200 m. Since all nodes can hear each other, no collision is
871 associated with ANN packets. The distributed MAC protocol
872 (DGR-SRORA) in Section IV is adopted. The ANN packets
873 are broadcast only for one round. In the simulation, six cases
874 of node-link pairs are considered: 10 nodes 15 links, 10 nodes
875 20 links, 20 nodes 30 links, 20 nodes 40 links, 30 nodes 45
876 links, and 30 nodes 60 links. For each case, the nodes are
877 randomly distributed and the links are randomly selected. The
878 traffic demand for each link is uniformly distributed within
879 $\{1, \dots, 128\}$ (units). 880

a) *Network throughput*: In each case of node-link pair, 881
the distributed protocol DGR-SRORA is compared with
882 SRTCWA and SRFCW. The network throughput of each case
883 is averaged over five tests and is shown in Fig. 8. In all
884 cases, our OFDMA-based channel-width adaptation scheme
885 outperforms SRTCWA and SRFCW. Moreover, compared with
886 the SRTCWA, DGR-SRORA improves the network throughput
887 by 14.3%, 20.0%, 18.5%, 15.0%, 13.3%, and 16.1%, respec-
888 tively, in six cases. As compared with SRFCW, DGR-SRORA
889 enhances the network throughput by 28.6%, 30.0%, 29.6%,
890 25.0%, 22.2%, and 24.2%, respectively, in six cases. 891

b) *Resource-allocation delay*: The total time required for
892 the distributed resource-allocation procedure is investigated. In
893 our simulation, the sum of the control subframe and the data
894

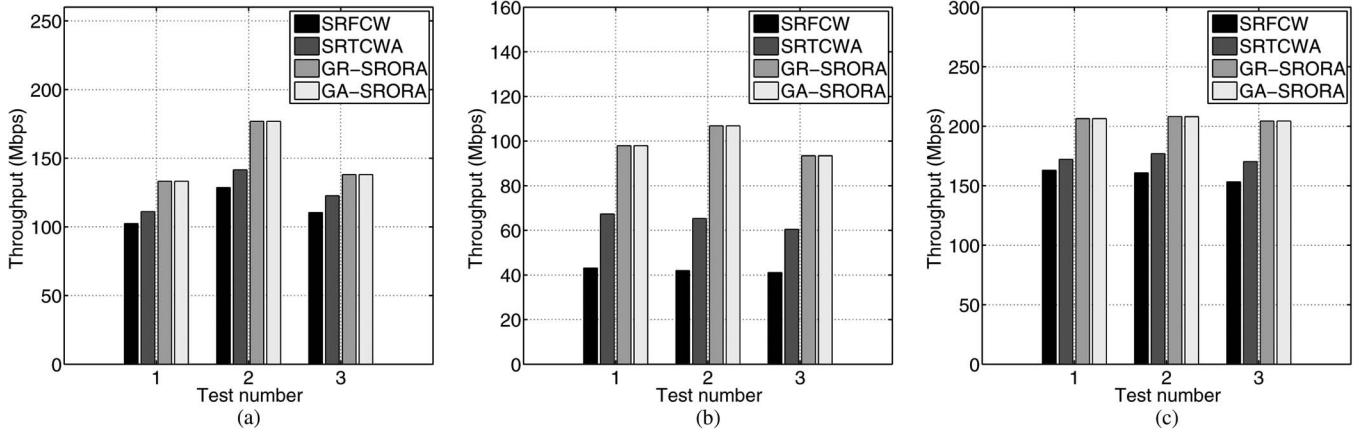


Fig. 7. Network throughput for simple topologies. (a) String topology. (b) Star topology. (c) Grid topology.

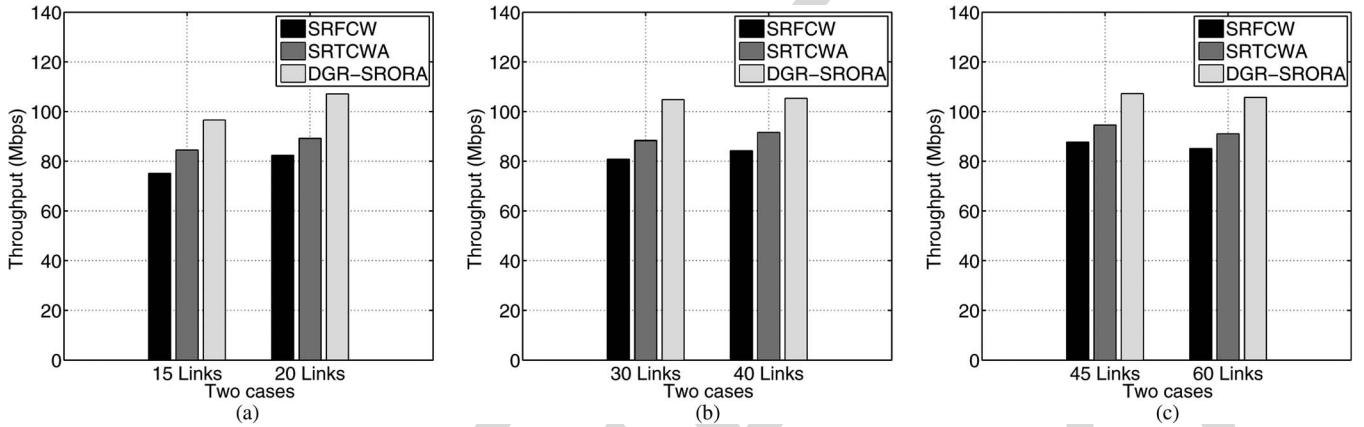


Fig. 8. Network throughput in the scenario of single interference domain. (a) 10 nodes. (b) 20 nodes. (c) 30 nodes.

TABLE I
TOTAL RESOURCE ALLOCATION TIME FOR THE SINGLE INTERFERENCE DOMAIN SCENARIO

Control Subframe	Data Subframe	Nodes: 10 Links: 15	Nodes: 10 Links: 20	Nodes: 20 Links: 30	Nodes: 20 Links: 40	Nodes: 30 Links: 45	Nodes: 30 Links: 60
20 ms	80 ms	9.2 ms	11.3 ms	18.4 ms	104.5 ms	112.1 ms	202.3 ms
15 ms	85 ms	9.2 ms	11.3 ms	103.9 ms	110.5 ms	202.4 ms	214.7 ms
10 ms	90 ms	9.2 ms	101.8 ms	200.5 ms	205.9 ms	305.7 ms	407.0 ms
5 ms	95 ms	104.0 ms	202.5 ms	304.7 ms	504.4 ms	801.5 ms	1100.5 ms

895 subframe (i.e., the length of a hybrid TDMA frame) is assumed 896 to be 100 ms. For each case of node-link pair, we consider 897 different lengths of control subframe and data subframe. The 898 results are shown in Table I. For each case of node-link pair, 899 when the control subframe is longer, the allocation delay is 900 smaller. Thus, if we need a faster allocation procedure, a larger 901 control subframe is necessary, which leads to more overhead in 902 signaling. However, even if the overhead is less than 10% for 903 signaling, the allocation can be done within 1 s for node-link 904 pairs: 10–15, 10–20, 20–30, 20–40, and 30–45. Such a fast 905 allocation procedure means that our MAC protocol is highly 906 adaptive to dynamic network conditions such as topology 907 change or traffic variations.

908 *Scenario of Multiple Interference Domains:* In this scenario, 909 50 nodes are randomly distributed in a square whose side 910 length is 1000 m, as shown in Fig. 9. The distributed MAC 911 protocol with modified ANN packet transmission in Section IV

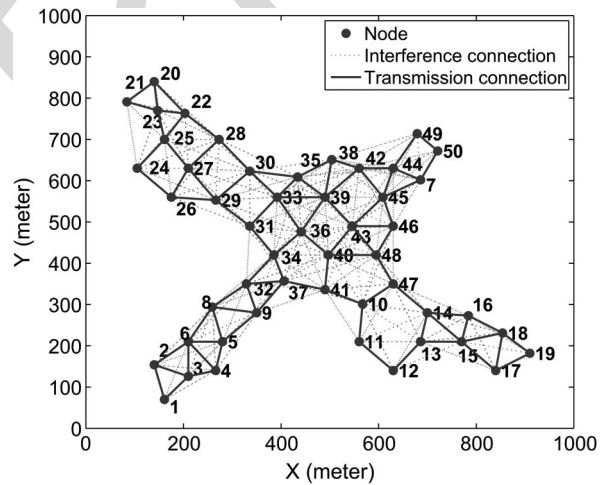


Fig. 9. Topology.

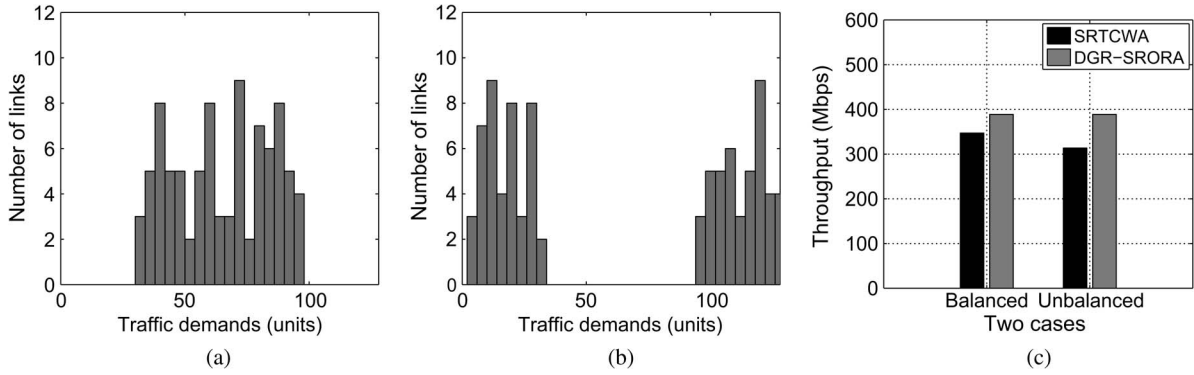


Fig. 10. Network throughput under different traffic distributions. (a) Balanced traffic distribution. (b) Unbalanced traffic distribution. (c) Network throughput.

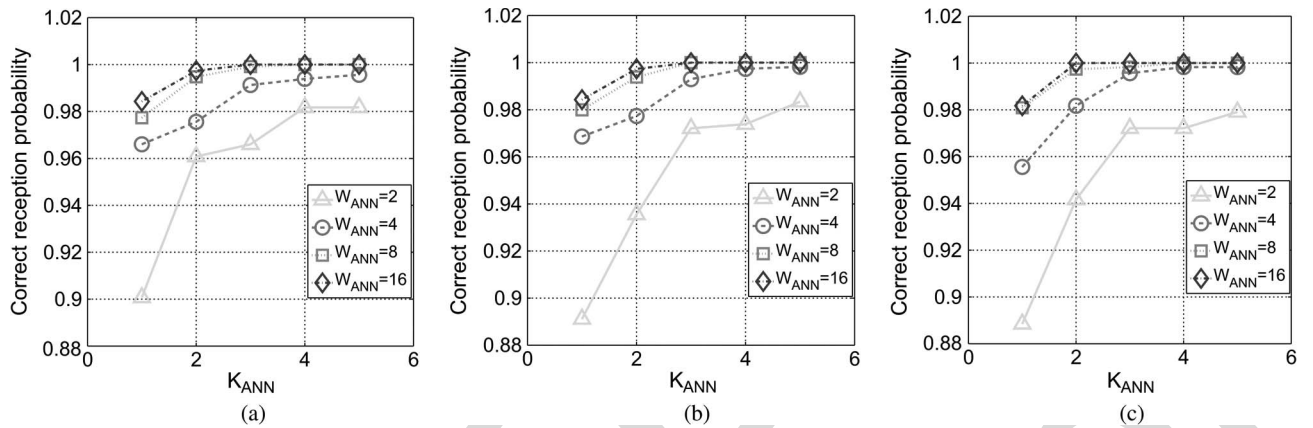


Fig. 11. ANN packet reception probability in the network with multiple interference domains. (a) Control subframe: 10 ms. (b) Control subframe: 15 ms. (c) Control subframe: 20 ms.

912 is adopted. In this protocol, the ANN packets are broadcast after 913 a randomly chosen waiting time for several rounds.

914 *c) Network throughput:* The impact of the traffic dis- 915 tribution to the network throughput is illustrated in Fig. 9. 916 Since there exists multiple interference domains, the distributed 917 protocol DGR-SROTSA may have allocation error due to col- 918 lision in ANN packets. Thus, we properly choose broadcasting 919 rounds and backoff window to reduce collisions. We randomly 920 choose 88 links in Fig. 9 for the test. Two cases with different 921 traffic distributions are considered. In the first case, the traffic 922 demand of each link is balanced and is uniformly distributed 923 in $\{32, \dots, 96\}$, as shown in Fig. 10(a). In the second case, 924 the traffic demand of each link is unbalanced and is uni- 925 formly distributed in either $\{1, 32\}$ or $\{96, 128\}$, as shown 926 in Fig. 10(b). The network throughputs of these two cases are 927 shown in Fig. 10(c). As compared with the traditional channel- 928 width adaptation scheme (i.e., SRTCWA), our MAC protocol 929 with OFDMA-based channel-width adaptation improves the 930 network throughput by 12% and 24%, respectively, in these two 931 cases. Higher throughput improvement is achieved in the case 932 of unbalanced traffic distribution because our MAC protocol 933 leverages OFDMA-based channel-width adaptation to allocate 934 resource in more proper way.

935 *d) Performance of the modified ANN packet broadcasting 936 mechanism:* In Section IV-D, we propose that an ANN packet

is broadcast after a randomly selected waiting time for several 937 rounds to reduce the collision probability. In this experiment, 938 this mechanism is investigated with respect to different broad- 939 casting rounds K_{ANN} and backoff window W_{ANN} . In Fig. 9, 940 we randomly choose 88 links for testing. Three cases (with 10-, 941 15-, and 20-ms control subframes) are considered. In each 942 case, the number of broadcasting rounds K_{ANN} varies from 943 1 to 5, and the broadcasting delay is randomly chosen in the 944 backoff window W_{ANN} . W_{ANN} is set 2, 4, 8, and 16 (the unit 945 is the transmission time of an ANN packet), respectively. The 946 reception probability of ANN packets is defined as the ratio 947 of the correctly received ANN packets over total transmitted 948 ANN packets. In Fig. 11, for the fixed K_{ANN} in all cases, 949 the correct reception probability is higher with larger W_{ANN} . 950 Similarly, for the fixed W_{ANN} , the correct reception probability 951 increases with a larger K_{ANN} . In each case, when $K_{ANN} = 952$ 3 and $W_{ANN} = 16$ or when $K_{ANN} = 4$ and $W_{ANN} = 8$, the 953 reception probability near reaches 1. 954

e) Resource-allocation delay: The total delay required 955 for the distributed resource-allocation procedure is also inves- 956 tigated. In our simulation, the sum of the control subframe and 957 the data subframe is assumed to be 100 ms, and three cases 958 (with 10-, 15-, and 20-ms control subframes) are considered. 959 The results are shown in Table II. When the control subframe is 960 longer, the allocation delay is smaller. Thus, if we need a faster 961

TABLE II
TOTAL RESOURCE ALLOCATION DELAY FOR THE SCENARIO OF MULTIPLE INTERFERENCE DOMAINS

Rounds	$W_{ANN}(10ms)^a$				$W_{ANN}(15ms)^b$				$W_{ANN}(20ms)^c$			
	2	4	8	16	2	4	8	16	2	4	8	16
$K_{ANN}=1$	0.20s	0.31s	0.50s	1.01s	0.11s	0.20s	0.31s	0.51s	0.10s	0.11s	0.21s	0.41s
$K_{ANN}=2$	0.21s	0.40s	0.71s	1.21s	0.20s	0.21s	0.41s	0.81s	0.11s	0.20s	0.31s	0.52s
$K_{ANN}=3$	0.31s	0.50s	0.91s	1.70s	0.20s	0.30s	0.51s	1.11s	0.12s	0.21s	0.40s	0.71s
$K_{ANN}=4$	0.40s	0.60s	1.21s	2.70s	0.21s	0.40s	0.61s	1.51s	0.20s	0.30s	0.51s	0.90s
$K_{ANN}=5$	0.50s	0.70s	1.31s	3.30s	0.30s	0.41s	0.80s	1.70s	0.21s	0.31s	0.52s	1.10s

^aThe length of the control subframe is 10 ms

^bThe length of the control subframe is 15 ms

^cThe length of the control subframe is 20 ms

962 allocation procedure, a larger control subframe is necessary,
963 which leads to more overhead in signaling. In each case, for
964 a fixed K_{ANN} , the allocation delay becomes larger as W_{ANN}
965 increases. Similarly, for a fixed W_{ANN} , the allocation delay
966 grows as K_{ANN} increases. For $K_{ANN} = 3$ and $W_{ANN} = 16$,
967 the maximum resource-allocation delay among three cases is
968 1.70 s (i.e., in the 10 ms control subframe case). For $K_{ANN} =$
969 4 and $W_{ANN} = 8$, the maximum resource-allocation delay
970 among three cases is 1.21 s (i.e., in the 10 ms control subframe
971 case). Therefore, with 10% signaling overhead (due to the
972 control subframe), the reception probability reaches 1 with a
973 resource-allocation delay of less than 2 s.

974

VI. CONCLUSION

975 In WMNs, there always exists a mismatch between link
976 capacity and traffic demand. In this paper, an OFDMA-based
977 channel-width adaptation mechanism has been designed to
978 alleviate such a mismatch of each link in WMNs. It was
979 formulated as a time slot and subchannel allocation problem
980 and was proved to be NP-complete. Thus, a greedy algorithm
981 and a GA were derived to obtain a suboptimal solution. Based
982 on the greedy algorithm, a distributed MAC protocol was de-
983 veloped to conduct channel-width adaptation for all links in the
984 WMN. Simulation results showed that the new MAC protocol
985 outperformed MAC protocols with traditional channel-width
986 adaptation. The channel-width adaptation mechanism studied
987 in this paper assumes that the traffic demand on each link is
988 given. In practice, traffic demand of a link is closely related
989 to MAC/routing cross-layer design. How to consider channel-
990 width adaptation under the framework of MAC/routing cross-
991 layer design is a key factor to further improve the network
992 performance of WMNs, which is an interesting topic for future
993 research.

994

REFERENCES

995 [1] R. Chandra, R. Mahajan, T. Moscibroda, R. Raghavendra, and P. Bahl, "A
996 case for adapting channel width in wireless networks," *ACM SIGCOMM*
997 *Comput. Commun. Rev.*, vol. 38, no. 4, pp. 135–146, 2008.
998 [2] L. Cheng, B. Henty, R. Cooper, D. Stancil, and F. Bai, "A measure-
999 ment study of time-scaled 802.11 a waveforms over the mobile-to-mobile
1000 vehicular channel at 5.9 GHz," *IEEE Commun. Mag.*, vol. 46, no. 5,
1001 pp. 84–91, May 2008.
1002 [3] T. Moscibroda, R. Chandra, Y. Wu, S. Sengupta, P. Bahl, and Y. Yuan,
1003 "Load-aware spectrum distribution in wireless LANs," in *Proc. IEEE*
1004 *ICNP*, 2008, pp. 137–146.

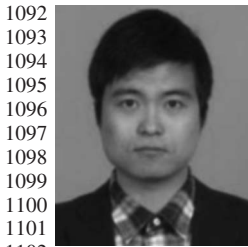
[4] P. Bahl, R. Chandra, T. Moscibroda, S. Narlanka, Y. Wu, and Y. Yuan, 1005
"Dynamic channel-width allocation in wireless networks," U.S. Patent 1006
8243 612, Aug. 14, 2012. 1007
[5] Y. Azar, A. Madry, T. Moscibroda, D. Panigrahi, and A. Srinivasan, 1008
"Maximum bipartite flow in networks with adaptive channel width," 1009
Theoretical Comput. Sci., vol. 412, no. 24, pp. 2577–2587, 1010
May 2011. 1011
[6] I. Akyildiz, X. Wang, and W. Wang, "Wireless mesh networks: A survey," 1012
Comput. Netw., vol. 47, no. 4, pp. 445–487, Mar. 2005. 1013
[7] D. Bharadia, E. McMillin, and S. Katti, "Full duplex radios," *Proc. ACM* 1014
SIGCOMM, pp. 375–386, 2013. 1015
[8] J. So and N. Vaidya, "Multi-channel MAC for ad hoc networks: Handling 1016
multi-channel hidden terminals using a single transceiver," in *Proc. 5th* 1017
ACM Int. Symp. MobiHoc, 2004, pp. 222–233. 1018
[9] R. Maheshwari, H. Gupta, and S. Das, "Multichannel MAC proto- 1019
cols for wireless networks," in *Proc. IEEE SECON*, 2006, vol. 2, 1020
pp. 393–401. 1021
[10] E. Aryafar, O. Gurewitz, and E. Knightly, "Distance-1 constrained chan- 1022
nel assignment in single radio wireless mesh networks," in *Proc. IEEE* 1023
Conf. INFOCOM, 2008, pp. 762–770. 1024
[11] A. Das, H. Alazemi, R. Vijayakumar, and S. Roy, "Optimization models 1025
for fixed channel assignment in wireless mesh networks with multiple 1026
radios," in *Proc. IEEE SECON*, 2005, pp. 463–474. 1027
[12] A. Subramanian, H. Gupta, S. Das, and J. Cao, "Minimum interference 1028
channel assignment in multiradio wireless mesh networks," *IEEE Trans.* 1029
Mobile Comput., vol. 7, no. 12, pp. 1459–1473, Dec. 2008. 1030
[13] X. Li, A. Nusairat, Y. Wu, Y. Qi, J. Zhao, X. Chu, and Y. Liu, 1031
"Joint throughput optimization for wireless mesh networks," *IEEE Trans.* 1032
Mobile Comput., vol. 8, no. 7, pp. 895–909, Jul. 2009. 1033
[14] K. Lee and V. Leung, "Fair allocation of subcarrier and power in an 1034
OFDMA wireless mesh network," *IEEE J. Sel. Areas Commun.*, vol. 24, 1035
no. 11, pp. 2051–2060, Nov. 2006. 1036
[15] H. Cheng and W. Zhuang, "Novel packet-level resource allocation with 1037
effective QoS provisioning for wireless mesh networks," *IEEE Trans.* 1038
Wireless Commun., vol. 8, no. 2, pp. 694–700, Feb. 2009. 1039
[16] A. Bayan and T. Wan, "A scalable QoS scheduling architecture for 1040
WiMAX multi-hop relay networks," in *Proc. 2nd ICETC*, 2010, vol. 5, 1041
pp. V5-326–V5-331. 1042
[17] S. Bai, W. Zhang, Y. Liu, and C. Wang, "Max–min fair scheduling in 1043
OFDMA-based multi-hop WiMAX mesh networks," in *Proc. IEEE ICC*, 1044
2011, pp. 1–5. 1045
[18] Y. Mai and K. Chen, "Design of zone-based bandwidth management 1046
scheme in IEEE 802.16 multi-hop relay networks," *EURASIP J. Wireless* 1047
Commun. Netw., no. 1, pp. 1–28, 2011. 1048
[19] S. Kim, X. Wang, and M. Madhian, "Optimal resource alloca- 1049
tion in multi-hop OFDMA wireless networks with cooperative relay," 1050
IEEE Trans. Wireless Commun., vol. 7, no. 5, pp. 1833–1838, 1051
May 2008. 1052
[20] K. Jain, J. Padhye, V. Padmanabhan, and L. Qiu, "Impact of interference 1053
on multi-hop wireless network performance," *Wireless Netw.*, vol. 11, 1054
no. 4, pp. 471–487, Jul. 2005. 1055
[21] M. Garey and D. Johnson, *Computers and Intractability: A Guide to* 1056
the Theory of NP-Completeness. San Francisco, CA, USA: Freeman, 1057
1979. 1058
[22] J. Bondy and U. Murty, *Graph Theory With Applications*. London, U.K.: 1059
MacMillan, 1976. 1060
[23] D. Johnson, "Worst case behavior of graph coloring algorithms," in *Proc.* 1061
5th Southeastern Conf. Combinatorics, Graph Theory Comput., 1974, 1062
pp. 513–527. 1063



Xudong Wang (SM'08) received the Ph.D. degree in electrical and computer engineering from Georgia Institute of Technology, Atlanta, GA, USA, in 2003.

He has been with several companies as a Senior Research Engineer, a Senior Network Architect, and an R&D Manager. He is currently with the University of Michigan-Shanghai Jiao Tong University (UM-SJTU) Joint Institute, Shanghai Jiao Tong University, Shanghai, China. He is a Distinguished Professor (Shanghai Oriental Scholar) and is the Director of the Wireless And Networking (WANG) Laboratory. He is also an affiliate faculty member with the Department of Electrical Engineering, University of Washington, Seattle, WA, USA. He has been actively involved in R&D, technology transfer, and commercialization of various wireless networking technologies. He holds several patents on wireless networking technologies, and most of his inventions have been successfully transferred to products. His research interests include wireless communication networks, smart grid, and cyber physical systems.

Dr. Wang was a voting member of the IEEE 802.11 and 802.15 Standards Committees. He is an Editor of the IEEE TRANSACTIONS ON VEHICULAR TECHNOLOGY, Elsevier's *Ad Hoc Networks*, and ACM/Kluwer's *Wireless Networks*. He has been a Guest Editor of several journals. He was the demo Co-Chair of the ACM International Symposium on Mobile Ad Hoc Networking and Computing (ACM MOBIHOC 2006), a Technical Program Co-chair of 2008 the Wireless Internet Conference (WICON) 2007, and a General Co-chair 2009 of WICON 2008. He has been a Technical Committee Member of many international conferences and a Technical Reviewer for numerous international journals and conferences.



Pengfei Huang received the B.E. degree in electrical engineering from Zhejiang University, Hangzhou, China, in 2010 and the M.S. degree in electrical engineering from Shanghai Jiao Tong University, Shanghai, China, in 2013. He is currently working toward the Ph.D. degree with the Department of Electrical and Computer Engineering, University of California at San Diego, La Jolla, CA, USA.

His current research interests are in the area of wireless communications and networking, with an emphasis on the design and performance analysis of real-time video transmission over wireless channel.



Jiang (Linda) Xie (SM'09) received the B.E. degree from Tsinghua University, Beijing, China, in 1997; the M.Phil. degree from The Hong Kong University of Science and Technology, Kowloon, Hong Kong, in 1999; and the M.S. and Ph.D. degrees from the Georgia Institute of Technology, Atlanta, GA, USA, in 2002 and 2004, respectively, all in electrical and computer engineering.

In August 2004, she joined the Department of Electrical and Computer Engineering, University of North Carolina, Charlotte (UNC-Charlotte), NC, USA, as an Assistant Professor. Currently, she is an Associate Professor. Her current research interests include resource and mobility management in wireless networks, quality-of-service provisioning, and next-generation Internet.

Dr. Xie is a Senior Member of the Association for Computing Machinery (ACM). She serves on the editorial boards of the IEEE TRANSACTIONS ON MOBILE COMPUTING, *IEEE Communications Surveys and Tutorial*, *Computer Networks* (Elsevier), the *Journal of Network and Computer Applications* (Elsevier), and the *Journal of Communications* (ETPub). She received the U.S. National Science Foundation Faculty Early Career Development (CAREER) Award in 2010, a Best Paper Award from the IEEE/Web Intelligence Congress/ACM International Conference on Intelligent Agent Technology (IAT 2010), and a Graduate Teaching Excellence Award from the College of Engineering from UNC-Charlotte in 2007.

Dr. Xie is a Senior Member of the Association for Computing Machinery (ACM). She serves on the editorial boards of the IEEE TRANSACTIONS ON MOBILE COMPUTING, *IEEE Communications Surveys and Tutorial*, *Computer Networks* (Elsevier), the *Journal of Network and Computer Applications* (Elsevier), and the *Journal of Communications* (ETPub). She received the U.S. National Science Foundation Faculty Early Career Development (CAREER) Award in 2010, a Best Paper Award from the IEEE/Web Intelligence Congress/ACM International Conference on Intelligent Agent Technology (IAT 2010), and a Graduate Teaching Excellence Award from the College of Engineering from UNC-Charlotte in 2007.



Mian Li received the B.E. and M.S. degrees from Tsinghua University, Beijing, China, in 1994 and 2001, respectively, and the Ph.D. degree from the University of Maryland, College Park, MD, USA, in 2007 with the Best Dissertation Award.

Currently, he is a tenure-track Assistant Professor with the University of Michigan-Shanghai Jiao Tong University (UM-SJTU) Joint Institute, Shanghai Jiao Tong University, Shanghai, China. Within the Mechanical Engineering Program at UM-SJTU Joint Institute, his research work has been focused on robust/

reliability-based multidisciplinary design optimization and sensitivity analysis, including topics such as multidisciplinary design optimization, robust/reliability design, sensitivity analysis, and approximation modeling.

AUTHOR QUERIES

AUTHOR PLEASE ANSWER ALL QUERIES

AQ1 = Please check if change made in this sentence is appropriate.

AQ2 = Semi-colon was changed to comma. Please check if appropriate.

AQ3 = The preceding statement is incomplete. Hence, it was combined with the subsequent sentence. Please check if appropriate.

END OF ALL QUERIES

IEEE
Proof